Predictor-Based Remote Tracking Control of a Mobile Robot

Alejandro Alvarez-Aguirre, *Member, IEEE*, Nathan van de Wouw, *Member, IEEE*, Toshiki Oguchi, *Member, IEEE*, and Henk Nijmeijer, *Fellow, IEEE*

***Abstract*— In this paper, we address the tracking control problem for a unicycle-type mobile robot which is remotely controlled by a two-channel, delay-inducing communication network. A predictor-based control strategy capable of controlling the negative effects of the time-delay is proposed. Moreover, conditions are provided guaranteeing the local or global asymptotic stability of the closed-loop system up to a maximum admissible delay. The applicability of the proposed predictor-controller combination is demonstrated using an interconnected robotic platform located partly in Eindhoven, the Netherlands, and Tokyo, Japan.**

***Index Terms*— Mobile robots, network-induced delays, predictive state estimation, tracking control over a network.**

I. Introduction

THE STUDY of robotic systems controlled by a communication network has become important to support designing of robots, which can perform remote, dangerous, and distributed tasks. Prospective applications include designing of, among others, underwater and space robots [1], [2], robots for agriculture, construction, and mining [3], [4], also the robots intended for hazardous environments or for search and rescue missions [5], [6].

In this paper, a control strategy that allows the remote tracking control of a unicycle-type mobile robot is proposed. Thus, the controller and the mobile robot are linked via a delay-inducing communication channel, which possibly compromises the performance and stability of the closed-loop system. The control scheme consists of a state predictor in combination with a tracking controller, which together control the negative effects of the network-induced delay. A schematic representation of the problem under study is shown in Fig. 1.

The problem of controlling a (robotic) system over a communication network has been addressed in different fields of control engineering. To properly place the contributions of the current paper in perspective, a concise overview of the literature in this field follows.

Manuscript received September 6, 2013; accepted December 17, 2013. Manuscript received in final form February 4, 2014. Date of publication April 3, 2014; date of current version October 15, 2014. Recommended by Associate Editor G. Antonelli.

A. Alvarez-Aguirre, N. van de Wouw, and H. Nijmeijer are with the Department of Mechanical Engineering, Eindhoven University of Technology, Eindhoven 5600 MB, The Netherlands (e-mail: a.alvarez.aguirre@ieee.com; n.v.d.wouw@tue.nl; h.nijmeijer@tue.nl).

T. Oguchi is with the Department of Mechanical Engineering, Tokyo Metropolitan University, Tokyo 192-0397, Japan (e-mail: t.oguchi@tmu.ac.jp).

Color versions of one or more of the figures in this paper are available online at http://ieeexplore.ieee.org.

Digital Object Identifier 10.1109/TCST.2014.2304741

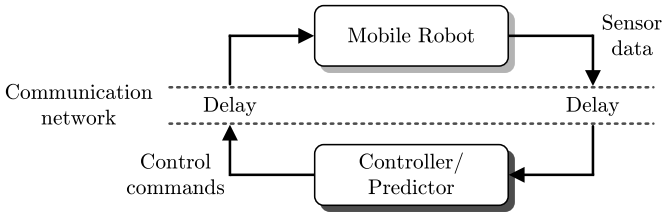

Fig. 1. Schematic representation of a mobile robot controlled by a delay-inducing communication network.

In the context of teleoperated robotic systems, several techniques have been proposed to overcome the negative effects of a network-induced delay (refer to [7] and [8] for an overview). Among the most common approaches are the operation under delay by shared compliant control or the addition of local force loops [9], [10], the use of the scattering transformation [11], a passivity-based approach [12], and wave variable transformations [13]. In a classical teleoperated system, both the local and remote sites are equipped with a controller, whereas in the current paper we consider the challenging scenario in which there is no controller on the remote site (see Fig. 1). We recognize the potential benefit of a controller at both the local and remote sites, as this becomes particularly important in safety-critical applications or applications with expensive equipment. Enforcing the passivity of the closed-loop system, such redundancy will allow the safe and stable teleoperation of a mobile robot with force reflection [14]. Nevertheless, it may not always be possible or cost effective to equip both sites with a controller. In this paper we, therefore, intend to show that not having a controller on the remote site is practically feasible even with a delay-inducing communication network in-between. This remote control architecture may be useful when considering the remote operation of multiple robots, such as, the control of a group of mobile robots with minimal sensing or decision-making capabilities from a remote command center [8] or the implementation of mobile sensor networks [15].

The stability analysis and the controller design for systems controlled over networks has received ample attention in the field of networked control systems (NCSs) [16]. This paper on NCSs is most devoted to the study of the effect of a wide range of network-induced impairments and uncertainties, such as (time-varying) network-induced delays, time-varying sampling intervals, packet losses, and other communication constraints, on closed-loop stability and performance. Currently, most

of the work in this field focuses on robust stability and stabilization, see, for example, [17] and [18] and many others. Of the few works in the NCSs literature that address the tracking control problem with time-varying delays, the vast majority focus on linear systems or small delays [19]–[21]. On the contrary, we consider the remote tracking problem (stabilization of time-varying trajectories) for a mobile robot with nonlinear dynamics (due to nonholonomic constraints) and employ a predictor-based control strategy to mitigate network-induced effects (with the delays being larger than the sampling interval, that is, so-called large delays). Motivated by measurements of Internet-induced delays conducted with remote sites, we consider the case of constant delays (refer to Section V-C for additional details).

In the current paper, we propose to solve the remote tracking control problem using a predictor-based state estimator. The origin of this type of predictor can be traced back to the appearance of the notion of anticipating synchronization in coupled chaotic systems, which was first observed by Voss in [22] for a scalar system and studied for a more general class of systems in [23]. As a result of this generalization, a synchronization-based state predictor for nonlinear systems with input time-delay (only) was proposed in [24].

A question that naturally arises is how the predictor proposed in this paper differs from the well-known Smith predictor [25] and its numerous extensions and applications (e.g., with nonlinear systems [26] and with discrete-time nonlinear systems [27]). First, the applicability of control strategies attributed to the classical Smith predictor has mostly been restricted to time-delayed linear systems and to (linearized) mechanical systems with regards to teleoperation (refer to [28] and [29] for respective surveys on these subjects). Second, a distinguishing feature of the synchronization-based predictor is that it encourages the convergence of the delayed state of the system and the delayed predicted state by a correction term (refer to Section III-C for additional details). This enables the predictor-controller combination to exhibit certain robustness against (additive, transient) perturbations to the system's inputs, as shown by the simulation results in Section VI. In contrast, the simplest implementation of the Smith predictor for nonlinear systems, such as in [26], does not provide a similar mechanism for convergence and disturbance rejection.

Recently, a number of predictor-based compensation techniques have been proposed for a broader class of nonlinear systems in [30] and [31]. These control strategies are inspired on the ideas behind the original Smith predictor and combine a state predictor together with a feedback control law designed for the delay-free system. Even though the remote tracking control strategy presented in this paper is based on a similar architecture as that in [30] and [31], the design procedure and the characteristics of the state predictors are quite different. On the one hand, the delay compensation strategy in [30] imposes no restrictions on the magnitude of the time-delay that can be compensated or on the size of the system's sampling period (it is a discrete-time implementation). Moreover, it can be applied to a relatively large class of nonlinear systems (although possibly requiring a numerical approximation of the predictor mapping to produce the predicted state). In addition, it employs so-called nominal feedback laws designed for the delay-free system [30]. On the other hand, the remote control strategy proposed in this paper has an upper bound on the maximum allowable time-delay and only under certain parameter restrictions it is capable of accommodating arbitrarily large delays (see Section IV). Moreover, it assumes to be a constant and known time-delay which poses certain restrictions on the reference trajectory (see Remark 10). Nevertheless, the current remote control strategy is fairly straightforward and easy to derive and implement. To begin with, it also employs a tracking control law designed for the delay-free system. In addition, the design of the state predictor can be rather straightforward owing to the fact that its structure very closely resembles that of a nonlinear observer. This simplicity in design facilitates an ease in implementation which is essential in practice, ultimately supporting an experimental validation in which the Internet is used as the communication channel in a robotic platform located partly in Eindhoven, the Netherlands, and in Tokyo, Japan. Additional simulations confirm the robustness of the proposed remote control strategy against certain perturbations, delay modeling errors, and time-varying delays (on time scales relevant to the closed-loop dynamics of the mobile robot).

The contribution of this paper is twofold. First, we propose a remote control strategy for a unicycle mobile robot, consisting of a tracking controller and a predictor, which guarantees the local or global stability of the resulting closed-loop system for delays smaller than a certain upper bound. Second, the control strategy is experimentally validated using an interconnected robotic platform located partly in the Netherlands and partly in Japan which uses the Internet as its communication channel. Some preliminary results regarding the control strategy proposed in this paper may be found in [32]. The main contributions of the current paper with respect to [32] are: 1) formal stability results and 2) novel simulation and experimental results validating the proposed remote control strategy.

The remainder of this paper is organized as follows. Section II provides preliminaries regarding the stability of retarded functional differential equations and delayed nonlinear cascaded systems. In Section III, the remote tracking control strategy for a unicycle robot is introduced. The local and global stability of the resulting closed-loop error dynamics is studied in Section IV. The experimental platform used in this paper is described in Section V. Illustrative simulation and experimental results are included in Section VI. Finally, this paper concludes with a discussion in Section VII.

Notation: The matrix sum norm, Frobenius norm, and induced matrix 1- and 2-norms of a matrix A are denoted as $\|A\|_{\text{sum}}$, $\|A\|_F$, $\|A\|_{i1}$, and $\|A\|_{i2}$, respectively. The minimum and maximum eigenvalues of a symmetric matrix A are given by $\lambda_{\min}(A)$ and $\lambda_{\max}(A)$, respectively. Throughout this paper there are a number of results in which there is no distinction regarding the vector norm being used. This means that these results hold for any valid vector norm as long as their use is consistent. In these cases, the vector norm will be denoted as $\|\cdot\|$.

II. Preliminaries

This section contains stability results employed in the remainder of this paper. To begin with, consider the following retarded functional differential equation (RFDE):

$$\dot{x}(t) = f(t, x_t) \tag{1}$$

where $f : \mathcal{D} \to \mathbb{R}^m$, $\mathcal{D} \subseteq (\mathbb{R} \times \mathcal{C}(m))$, and $\mathcal{C}(m) = \mathcal{C}([-\tau, 0], \mathbb{R}^m)$ is the (Banach) space of continuous functions mapping the interval $[-\tau, 0]$ into $\mathbb{R}^m$. This vector space is equipped with the norm $\|\cdot\|_c$, denoted as the continuous norm, which is defined for a function $\varphi \in \mathcal{C}([a, b], \mathbb{R}^m)$ as $\|\varphi\|_c = \max_{a \le s \le b} \|\varphi(s)\|$, where $\|\cdot\|$ denotes any vector norm. In (1), $t \in \mathbb{R}$, $x(t) \in \mathbb{R}^m$, and $x_t \in \mathcal{C}(m)$ is defined as $x_t(s) = x(t + s)$, for $-\tau \le s \le 0$.

We have that the function x is a solution of (1) given by $x(t; t_0, \phi)$, where $x_{t_0} = \phi$ denotes the initial condition of the system. In addition, for any $\varphi \in \mathcal{C}(m)$, that is, any element of the Banach space, let $\varphi(0) \in \mathbb{R}^m$ and $\varphi(-\tau) \in \mathbb{R}^m$ denote φ at the end and beginning of the interval $[-\tau, 0]$, respectively, and, generically, let $\varphi(s) \in \mathbb{R}^m$ denotes φ at $s \in [-\tau, 0]$. The functional f in (1) is assumed to be continuous on each set of the form $\mathbb{R}^+ \times \mathcal{C}_\rho(m)$, where $\rho > 0$, $\mathcal{C}_\rho(m) = \{\varphi \in \mathcal{C}(m) : \|\varphi\|_c < \rho\}$, bounded by some constant $M(\rho)$, and Lipschitz with some constant $L(\rho)$. We also assume that $f(t, 0) = 0$, for all $t \in \mathbb{R}^+$, such that system (1) has a zero equilibrium state.

A particular type of RFDE of special interest in this paper is the following nonlinear cascaded system:

$$\dot{x}(t) = f_x(t, x_t) + g_{xy}(t, x_t, y_t) \tag{2a}$$

$$\dot{y}(t) = f_y(t, y_t) \tag{2b}$$

where $x \in \mathbb{R}^m$, $y \in \mathbb{R}^n$, $x_t \in \mathcal{C}(m)$, and $y_t \in \mathcal{C}(n)$. We assume that $f_y(t, 0) = 0$, $f_x(t, 0) = g_{xy}(t, \varphi_x, 0) = 0$ for all $t \in \mathbb{R}^+$ and $\varphi_x \in \mathcal{C}(m)$, such that the system has the zero equilibrium state. In the absence of the coupling term $g_{xy}(t, x_t, y_t)$, system (2a) takes the following form:

$$\dot{x}(t) = f_x(t, x_t) \tag{3}$$

denoted hereinafter as the x-dynamics without coupling.

The following theorems formulate sufficient conditions to establish the local and global uniform asymptotic stability of the nonlinear delayed cascaded system (2). The stability definitions for RFDEs used in these theorems may be found in the classical works of [33, Ch. 1, Def. 1.1] and [34, Ch. 5, Def. 1.1].

Theorem 1 [35, Th. 2]: Consider the nonlinear delayed cascaded system (2) and let both the zero solution of the x-dynamics without coupling (3) and the y-dynamics in (2b) be locally uniformly asymptotically stable (LUAS). Then, $[x^T\ y^T]^T = 0$ is a LUAS equilibrium point of system (2).

Theorem 2 [36, Th. 4]: Assume that for system (3) there exists a function $V(t, x)$ of the Lyapunov-Razumikhin type which satisfies the following assumptions:

1) $V(t, x)$ is continuously differentiable, positive definite, and has the infinitesimal upper limit with $\|x\| \to 0$ and the infinitely great lower limit with $\|x\| \to \infty$;
2) the time-derivative of the function V, given by the functional $\dot{V}(t, \varphi_x) = \partial V/\partial t(t, \varphi_x(0)) + \partial V/\partial x(t, \varphi_x(0)) f_x(t, \varphi_x)$, satisfies the estimate $\dot{V}(t, \varphi_x) \le 0$ for all $\varphi_x \in \Omega_t(V) = \{\varphi \in \mathcal{C}(m) : \max\_\tau \le s \le 0 V(t + s, \varphi_x(s)) \le V(t, \varphi_x(0))\}$;
3) $|\dot{V}(t, \varphi_x)| \ge U(t, \varphi_x)$ for all $(t, \varphi_x) \in \mathbb{R}^+ \times \mathcal{C}(m)$, where the functional $U(t, \varphi_x)$ is uniformly continuous and bounded in each set of the form $\mathbb{R}^+ \times \mathcal{K}$ with a compact set $\mathcal{K} \subset \mathcal{C}$;
4) the intersection of the sets $V_{\max}^{-1}(\infty, c) := \{\varphi_x \in \mathcal{C}(m) | \exists \varphi_n \to \varphi_x, t_n \to +\infty : \lim_{n\to\infty} \max_{-\tau \le s \le 0} V(t_n + s, \varphi_n(s)) = \lim_{n\to\infty} V(t_n, \varphi_n(0)) = c\}$ and $U^{-1}(\infty, 0)$ is empty with $c \ne 0$;
5) for all $x \in \mathbb{R}^m$ such that $\|x\| > \eta$, the inequality $\|\partial V/\partial x\| \cdot \|x\| \le c_1 V(t, x)$ holds, and, for all $x \in \mathbb{R}^m$ such that $\|x\| \le \eta$, the estimate $\|\partial V/\partial x\| \le c$ is valid with certain constants $\eta, c_1, c > 0$;

and that additionally the following conditions are satisfied:

6) for $\varphi_y \in \mathcal{C}(n)$ and some continuous functions $\alpha_1, \alpha_2 : \mathbb{R}^+ \to \mathbb{R}^+$ the functional g_{xy} in (2a) admits the following estimate:

$$\|g_{xy}(t, \varphi_x, \varphi_y)\| \le (\alpha_1(\|\varphi_y\|_c) + \alpha_2(\|\varphi_y\|_c)\|\varphi_x(0)\|)\|\varphi_y\|_c;$$

7) solutions of system (2b) admit the estimate $\|y(t; t_0, \phi_y)\| \le k_1 \|\phi_y\|_c e^{-k_2 t}$ with certain constants $k_1, k_2 > 0$.

Then, $[x^T\ y^T]^T = 0$ is a globally uniformly asymptotically stable equilibrium point of system (2).

Remark 3: From [36, Remarks 2 and 3], we have that if the function $V(t, x)$ is quadratic in x, the bounds on its growth posed in the fifth condition are automatically satisfied and $\|\varphi_x(0)\|$ can be replaced by $\|\varphi_x\|_c$ in the estimation of the functional g_{xy} in the sixth assumption.

The following definition will be useful when investigating the stability of the proposed remote control strategy.

Definition 4 [37, Def. 2.3.5]: A continuous function $\psi : \mathbb{R}^+ \to \mathbb{R}$ is said to be persistently exciting (PE) if all of the following conditions hold:

1) a constant $K > 0$ exists such that $|\psi(t)| \le K$, $\forall t \ge 0$;
2) a constant $L > 0$ exists such that $|\psi(t) - \psi(t')| \le L|t - t'|$, $\forall t, t' \ge 0$;
3) constants $\delta > 0$ and $\epsilon > 0$ exist such that $\forall t \ge 0$, $\exists s : t - \delta \le s \le t$ such that $|\psi(s)| \ge \epsilon$.[1]

III. Remote Tracking Control Strategy

In this section, we propose a predictor-controller combination to address the remote tracking control problem, to be formalized below.

A. Unicycle-Type Mobile Robot and Problem Setting

Consider a unicycle mobile robot as shown schematically in Fig. 2. The position at time t of point P with respect to

[1] This condition implies that within the interval $[t - \delta, t]$, there exists a time instant s at which the absolute value of $\psi(s)$ is equal to or greater than a certain $\epsilon > 0$.

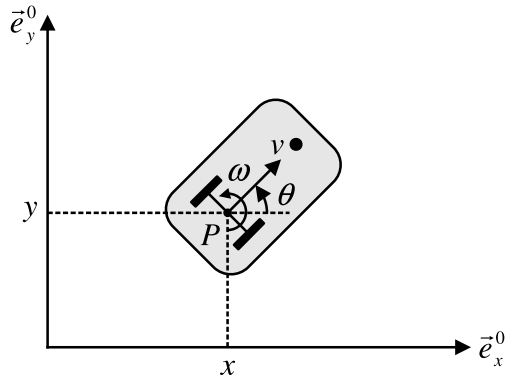

Fig. 2. Schematic representation of a unicycle-type mobile robot.

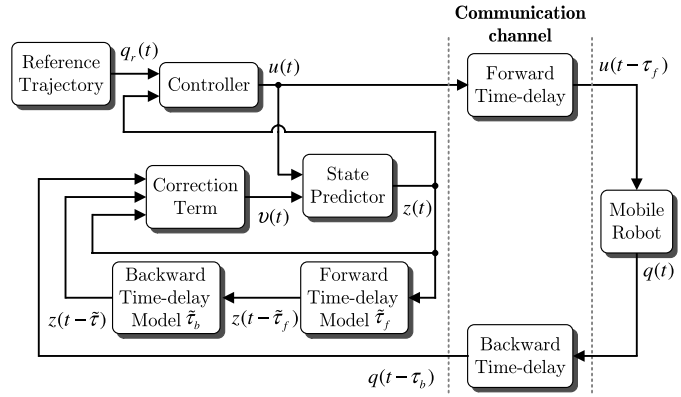

Fig. 3. Block diagram representation of the remote tracking control strategy.

the global coordinate frame $\underline{\vec{e}}^{\,0} = [\vec{e}_x^{\,0} \;\; \vec{e}_y^{\,0}]^T$ is denoted by the coordinates $(x(t), y(t))$, whereas the angle at time t between the heading direction of the robot and the $\vec{e}_x^{\,0}$-axis of the global coordinate frame is denoted by $\theta(t)$. The delay-free posture kinematic model of the unicycle is given by

$$\dot{x}(t) = v(t)\cos\theta(t) \tag{4a}$$
$$\dot{y}(t) = v(t)\sin\theta(t) \tag{4b}$$
$$\dot{\theta}(t) = \omega(t) \tag{4c}$$

where $v(t)$ and $\omega(t)$ are the translational and rotational velocities of the robot, respectively, and are regarded as its control inputs. The state of the system is denoted by $q(t) = [x(t)\, y(t)\, \theta(t)]^T$ and its control inputs are grouped into $u(t) = [v(t)\, \omega(t)]^T$.

In the tracking control problem, the control objective of the robot is to track the reference position $(x_r(t), y_r(t))$ with the reference orientation $\theta_r(t)$. The reference orientation and translational and rotational velocities of the robot are defined as follows:

$$\theta_r(t) = \operatorname{atan2}(\dot{y}_r(t), \dot{x}_r(t)) \tag{5a}$$
$$v_r(t) = \sqrt{\dot{x}_r^2(t) + \dot{y}_r^2(t)} \tag{5b}$$
$$\omega_r(t) = \frac{\dot{x}_r(t)\ddot{y}_r(t) - \ddot{x}_r(t)\dot{y}_r(t)}{\dot{x}_r^2(t) + \dot{y}_r^2(t)} = \dot{\theta}_r(t). \tag{5c}$$

As stated by [38], in order for the tracking problem to be soluble, $\theta_r(t)$ should satisfy (5a) and there must exist reference translational and rotational velocities $v_r(t)$ and $\omega_r(t)$ which satisfy (5b) and (5c), respectively. The associated reference state trajectory is denoted by $q_r(t) = [x_r(t)\, y_r(t)\, \theta_r(t)]^T$.

In the current problem setting, the mobile robot is subject to a network-induced bilateral time-delay consisting of a forward and a backward time-delay (see Fig. 3). The inputs of the mobile robot are subject to the forward time-delay τ_f, resulting in the following posture kinematic model:

$$\dot{x}(t) = v(t-\tau_f)\cos\theta(t) \tag{6a}$$
$$\dot{y}(t) = v(t-\tau_f)\sin\theta(t) \tag{6b}$$
$$\dot{\theta}(t) = \omega(t-\tau_f). \tag{6c}$$

The outputs of the mobile robot are subject to the output time-delay τ_b, yielding the measured state $q(t-\tau_b) = [x(t-\tau_b)\; y(t-\tau_b)\; \theta(t-\tau_b)]^T$. The round-trip time-delay is defined as $\tau := \tau_b + \tau_f$. We adopt the following assumption on the delay.

Assumption 1: The delay τ is assumed to be constant and known.

We note that this assumption is employed in the stability analyses pursued in Section IV. Delay measurements presented in Section V validate this assumption on the delay, at least on time scales relevant to the (closed-loop) dynamics of the mobile robot. In Section VI, however, we present simulation and experimental results that confirm the robustness of the control strategy, proposed below, for uncertain and time-varying delays.

Let us now state the tracking control problem that we aim to solve.

Given the unicycle robot (6) subject to a network-induced delay $\tau = \tau_f + \tau_b$, design a (predictor-based) tracking control law such that the mobile robot tracks a (possibly delayed) version of the reference trajectory $q_r(t)$.

B. State Predictor Design

To solve the remote tracking control problem for a unicycle-type mobile robot, we propose the predictor-controller combination shown in Fig. 3. The state predictor, with state $z(t) = [z_1(t)\, z_2(t)\, z_3(t)]^T$, is designed as follows:

$$\dot{z}_1(t) = v(t)\cos z_3(t) + \nu_x(t) \tag{7a}$$
$$\dot{z}_2(t) = v(t)\sin z_3(t) + \nu_y(t) \tag{7b}$$
$$\dot{z}_3(t) = \omega(t) + \nu_\theta(t) \tag{7c}$$

in which the robot kinematics can clearly be recognized and where $\nu(t) = [\nu_x(t)\, \nu_y(t)\, \nu_\theta(t)]^T$ is a correction term based on the predicted and the measured states. To design the correction term $\nu(t)$, a set of error coordinates $p_e(t)$ which relate the difference between the delayed predicted state $z(t-\tilde{\tau})$ and the delayed system state $q(t-\tau_b)$ is introduced

$$p_e(t) = \begin{bmatrix} p_{1_e}(t) \\ p_{2_e}(t) \\ p_{3_e}(t) \end{bmatrix} = R_{p_e}(t-\tilde{\tau}) \begin{bmatrix} x(t-\tau_b) - z_1(t-\tilde{\tau}) \\ y(t-\tau_b) - z_2(t-\tilde{\tau}) \\ \theta(t-\tau_b) - z_3(t-\tilde{\tau}) \end{bmatrix} \tag{8}$$

with

$$R_{p_e}(t-\tilde{\tau}) = \begin{bmatrix} \cos z_3(t-\tilde{\tau}) & \sin z_3(t-\tilde{\tau}) & 0 \\ -\sin z_3(t-\tilde{\tau}) & \cos z_3(t-\tilde{\tau}) & 0 \\ 0 & 0 & 1 \end{bmatrix}$$

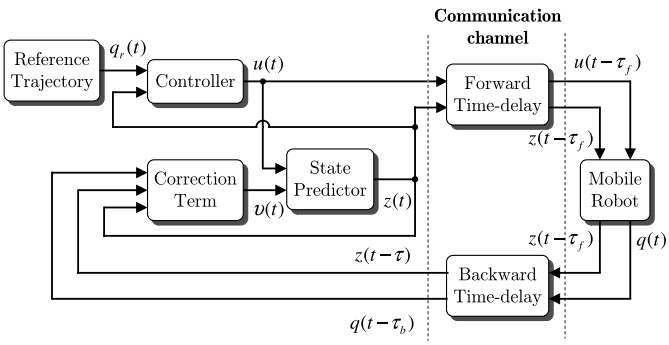

Fig. 4. Modified block diagram representation of the remote tracking control strategy considering signal bouncing.

where $\tilde{\tau} := \tilde{\tau}_f + \tilde{\tau}_b$ is the sum of the modeled input and output network-induced delays.

Remark 6: The proposed state predictor requires an accurate model of the network-induced delay, because predictor-like control strategies tend to be sensitive to mismatches in the delay model [7], [39]. A straightforward approach to obtain an estimate $\tilde{\tau}$ of the real delay τ is to measure the communication delay. This has been done in Section V-C, where the round-trip delay time of an Internet connection between the Netherlands and Japan, used for the remote tracking control task, has been measured at approximately 268 ms. The measurements in Section V-C show that the round-trip delay is fairly constant and reproducible. Thus, for the problem setting in this paper, we consider the constant delays and assume the availability of an accurate estimate $\tilde{\tau}$ of the real delay τ. An alternative approach for the measurement-based modeling of the time-delay is called signal bouncing. In this case, the remote tracking control strategy is modified, resulting in the block diagram representation shown in Fig. 4. Using the communication channel to delay the predicted state, is no longer necessary to model the time-delay.

As the time-delay is assumed to be known (see Remark 6), we have that $\tilde{\tau}_f = \tau_f$ and $\tilde{\tau}_b = \tau_b$, which yields $\tilde{\tau} = \tau$. The prediction error $p_e(t)$ in (8) is due to the difference between the delayed predicted state and the delayed system state, that is, $q(t-\tau_b) - z(t-\tilde{\tau})$. Consequently, if the prediction error $p_e(t)$ converges to zero, the predictor anticipates the state of the system by a time τ_f.

With the error coordinates (8), the correction term $\nu(t) = [\nu_x(t)\, \nu_y(t)\, \nu_\theta(t)]^T$ is designed as follows:

$$\nu_x(t) = k_x p_{1_e}(t) \cos z_3(t) - k_y p_{2_e}(t) \sin z_3(t) \tag{9a}$$

$$\nu_y(t) = k_x p_{1_e}(t) \sin z_3(t) + k_y p_{2_e}(t) \cos z_3(t) \tag{9b}$$

$$\nu_\theta(t) = k_\theta p_{3_e}(t) \tag{9c}$$

where k_x, k_y, and k_θ are the correction gains.

Remark 7: The prediction error (8) and correction term (9) are designed such that, once the tracking control law is proposed (see Section III-C), the resulting closed-loop error dynamics possess a cascaded structure (see Section IV). This feature is instrumental for the ensuing stability analysis, as it allows using Theorems 1 and 2, respectively, as a basis for the local and global stability analysis of the closed-loop system.

C. Tracking Controller Design

The tracking control problem described in Section III-A can now be formulated as follows.

Given the unicycle robot (6) subject to a network-induced delay $\tau = \tau_f + \tau_b$ and the state estimator (7)–(9), design a tracking control law such that the mobile robot tracks a delayed version $q_r(t-\tau_f)$ of the reference trajectory.

Given this control goal, we can formulate the objective of the predictor-controller combination as having the state of the unicycle converge to the state of the reference trajectory delayed by τ_f, that is, $q(t) \to q_r(t-\tau_f)$ as $t \to \infty$. A way to reach this objective is to build a predictor in which the predicted state anticipates the state of the unicycle by τ_f, that is, $z(t) \to q(t+\tau_f)$ as $t \to \infty$.

Considering the requirement on the state predictor described above, a second set of error coordinates $z_e(t)$ related to the difference between the predicted state $z(t)$ and the reference trajectory $q_r(t)$ is defined as follows:

$$z_e(t) = \begin{bmatrix} z_{1_e}(t) \\ z_{2_e}(t) \\ z_{3_e}(t) \end{bmatrix} = R_{z_e}(t) \begin{bmatrix} x_r(t) - z_1(t) \\ y_r(t) - z_2(t) \\ \theta_r(t) - z_3(t) \end{bmatrix} \tag{10}$$

with

$$R_{z_e}(t) = \begin{bmatrix} \cos z_3(t) & \sin z_3(t) & 0 \\ -\sin z_3(t) & \cos z_3(t) & 0 \\ 0 & 0 & 1 \end{bmatrix}.$$

The control scheme in Fig. 3 shows that the output of the state predictor constitutes the input of the tracking controller. Here, we employ the tracking control law proposed in [40] in combination with the state predictor state estimator (7)–(9). Hence, the control law uses the predicted error coordinates $z_e(t)$ as defined in (10), which yields

$$v(t) = v_r(t) + c_x z_{1_e}(t) - c_y \omega_r(t) z_{2_e}(t), \quad c_x > 0, \quad c_y > -1 \tag{11a}$$

$$\omega(t) = \omega_r(t) + c_\theta z_{3_e}(t), \quad c_\theta > 0. \tag{11b}$$

Because of the input time-delay, the control action applied to the unicycle in (6) is given by

$$\begin{aligned} v(t-\tau_f) &= v_r(t-\tau_f) + c_x z_{1_e}(t-\tau_f) \\ &\quad - c_y \omega_r(t-\tau_f) z_{2_e}(t-\tau_f) \end{aligned} \tag{12a}$$

$$\omega(t-\tau_f) = \omega_r(t-\tau_f) + c_\theta z_{3_e}(t-\tau_f). \tag{12b}$$

The resulting control inputs hint at how the system behaves. Intuitively, if the errors $p_e(t)$ and $z_e(t)$ converge to zero, the robot state $q(t)$ converges to the delayed reference state trajectory $q_r(t-\tau_f)$. This claim will be further examined in the next section.

IV. Stability Analysis

To guarantee that the tracking control problem introduced in Section III-C is solved, it is sufficient to prove the asymptotic stability of the equilibrium point $(z_e^T, p_e^T)^T = 0$ of the closed-loop error dynamics of the predictor-controller combination. This section presents these closed-loop error dynamics, together with theorems which pose sufficient conditions for their local and global uniform asymptotic stability.

A. Closed-Loop Error Dynamics

Exploiting the predictor (7), correction term (9), and control law (12), and considering the state definitions $\xi_1(t) := [z_{1_e}(t)\, z_{2_e}(t)\, p_{1_e}(t)\, p_{2_e}(t)]^T$ and $\xi_2(t) := [z_{3_e}(t)\, p_{3_e}(t)]^T$, the resulting closed-loop error dynamics may be represented as the following cascaded system:

$$\dot{\xi}_1(t) = A_1(t, t-\tau)\xi_1(t) + A_2\xi_1(t-\tau) + g(t, \xi_{1_t}, \xi_{2_t}) \tag{13a}$$

$$\dot{\xi}_2(t) = B_1\xi_2(t) + B_2\xi_2(t-\tau) \tag{13b}$$

where ξ_{i_t}, $i = 1, 2$, is an element of the Banach space $\mathcal{C}(l_i) = C([-\tau, 0], \mathbb{R}^{l_i})$, with $l_1 = 4$ and $l_2 = 2$, defined by $\xi_{i_t}(s) := \xi_i(t+s)$ for $s \in [-\tau, 0]$. The matrices in (13) are given by

$$A_1(t, t-\tau) = \begin{bmatrix} -c_x & (1+c_y)\omega_r(t) & -k_x & 0 \\ -\omega_r(t) & 0 & 0 & -k_y \\ 0 & 0 & 0 & \omega_r(t-\tau) \\ 0 & 0 & -\omega_r(t-\tau) & 0 \end{bmatrix} \tag{14a}$$

$$A_2 = \begin{bmatrix} 0 & 0 & 0 & 0 \\ 0 & 0 & 0 & 0 \\ 0 & 0 & -k_x & 0 \\ 0 & 0 & 0 & -k_y \end{bmatrix} \tag{14b}$$

$$B_1 = \begin{bmatrix} -c_\theta & -k_\theta \\ 0 & 0 \end{bmatrix}, \qquad B_2 = \begin{bmatrix} 0 & 0 \\ 0 & -k_\theta \end{bmatrix} \tag{14c}$$

$$g(t, \xi_{1_t}, \xi_{2_t}) = \begin{bmatrix} g_{11} & k_\theta z_{2_e}(t) \\ g_{21} & -k_\theta z_{1_e}(t) \\ 0 & g_{32} \\ 0 & g_{42} \end{bmatrix} \xi_2(t) + \begin{bmatrix} 0 & 0 \\ 0 & 0 \\ c_\theta p_{2_e}(t) & k_\theta p_{2_e}(t) \\ -c_\theta p_{1_e}(t) & -k_\theta p_{1_e}(t) \end{bmatrix} \xi_2(t-\tau) \tag{14d}$$

with

$$g_{11} = c_\theta z_{2_e}(t) - v_r(t)\int_0^1 \sin(s z_{3_e}(t))ds \tag{15a}$$

$$g_{21} = -c_\theta z_{1_e}(t) + v_r(t)\int_0^1 \cos(s z_{3_e}(t))ds \tag{15b}$$

$$g_{32} = -(v_r(t-\tau) + c_x z_{1_e}(t-\tau) - c_y\omega_r(t-\tau)z_{2_e}(t-\tau))\int_0^1 \sin(s p_{3_e}(t))ds \tag{15c}$$

$$g_{42} = (v_r(t-\tau) + c_x z_{1_e}(t-\tau) - c_y\omega_r(t-\tau)z_{2_e}(t-\tau))\int_0^1 \cos(s p_{3_e}(t))ds \tag{15d}$$

where the following equalities:

$$\int_0^1 \cos(sx)ds = \begin{cases} \frac{\sin x}{x} & \text{for} \quad x \neq 0 \\ 1 & \text{for} \quad x = 0 \end{cases} \tag{16a}$$

$$\int_0^1 \sin(sx)ds = \begin{cases} \frac{1-\cos x}{x} & \text{for} \quad x \neq 0 \\ 0 & \text{for} \quad x = 0 \end{cases} \tag{16b}$$

have been used in the definition of g_{11}, g_{21}, g_{32}, and g_{42}.

B. Local Asymptotic Stability

The following theorem formulates sufficient conditions under which $(z_e^T, p_e^T)^T = 0$ is a LUAS equilibrium point of (13).

Theorem 8: Consider the posture kinematic model of a unicycle robot subject to a constant input time-delay τ_f, as given by (6). The reference position of the robot is given by $(x_r(t), y_r(t))$, whereas its reference orientation $\theta_r(t)$ is given by (5a). Additionally, consider the tracking controller as given in (5b), (5c), (10), and (11). Moreover, consider the state predictor (7)–(9). If the following conditions are satisfied:

1) the reference translational velocity $v_r(t)$ is bounded;
2) the reference rotational velocity $\omega_r(t)$ is persistently exciting;
3) the tracking gains satisfy $c_x, c_\theta > 0, c_y > -1$;
4) the correction gains satisfy $k_x = k_y = k > 0, k_\theta > 0$;
5) Assumption 1 is satisfied, which implies that $\tilde{\tau} = \tau = \tau_b + \tau_f$;
6) the time-delay τ belongs to the interval $0 \leq \tau < \tau_{\max}$, with

$$\tau_{\max} = \min\left\{\frac{\pi}{2k_\theta}, \frac{1}{\sqrt{p}(\bar{\omega}_r + k)}\right\} \tag{17}$$

where $p > 1$ and $\bar{\omega}_r = \sup_{t\in\mathbb{R}} |\omega_r(t)|$

then, $(z_e^T, p_e^T)^T = 0$ is a LUAS equilibrium point of the closed-loop error dynamics (13).

Proof: The proof is given in Appendix A. ■

Remark 9: Under the conditions of Theorem 8, we have that $z(t) \to q(t+\tau_f)$ as $t \to \infty$, that is, the predicted state anticipates the state of the system by τ_f, and $q(t) \to q_r(t-\tau_f)$ as $t \to \infty$, that is, the system tracks the reference trajectory delayed by τ_f. However, if the reference trajectory is available in advance and the value of the forward time-delay is known, the predictor-controller combination (7)–(11) can employ knowledge on $v_r(t+\tau_f)$, $\omega_r(t+\tau_f)$, and $q_r(t+\tau_f)$, which will result in the mobile robot tracking the (nondelayed) desired reference trajectory $q_r(t)$.

Remark 10: The persistency of excitation condition on $\omega_r(t)$ in Theorem 8 prevents the mobile robot from following a straight line (see Def. 4). This practical limitation is related to the usage of the tracking control law (taken from [40]) in the predictor-controller combination and is not a result of the remote control strategy proposed. For additional details on this limitation and possible options to overcome it, refer to [37, Ch. 4].

Given the upper bound on the delay in (17), the left-most plot in Fig. 5 shows the maximum allowable time-delay satisfying $\tau < \pi/2k_\theta$ given different values for the correction gain k_θ. The middle plot in Fig. 5 shows the maximum allowable time-delay satisfying $\tau < 1/\sqrt{p}(\bar{\omega}_r + k)$ considering $p = 1$ and different values for the correction gain k and the maximum absolute reference rotational velocity $\bar{\omega}_r$.

The delay bound in the left-most plot has been obtained by spectral analysis of characteristic equation of a first-order linear system with delay [(28b) in Appendix A], whereas the delay bound in the middle plot is a result of the Lyapunov-Razumikhin analysis of a second-order linear system with

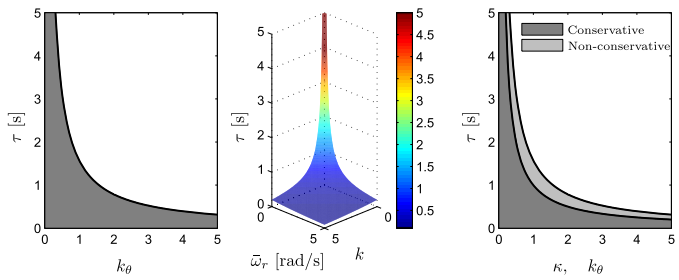

Fig. 5. Left and center plots: allowable time-delay τ given the two conditions in (17) (the allowable delay has been cut off at 5 [s]); right plot: comparison between the conservative and nonconservative delay bounds in (17) considering $\kappa := \bar{\omega}_r + k$ for the conservative bound.

delay [(18b) in Appendix A]. Hence, only the computation of the latter bound introduces conservativeness [33], [34]. The right-most plot in Fig. 5 shows a graphical comparison between both delay bounds considering $p = 1$ and different values of the unique parameter $\kappa := \bar{\omega}_r + k$ for the conservative bound. The plot provides an idea of the conservativeness introduced by the use of the Lyapunov-Razumikhin approach to analyze the stability of (part of) the system. Furthermore, it shows that lowering the robot's maximum reference rotational velocity $\bar{\omega}_r$ and/or its correction gains k_x, k_y should allow for the compensation of a time-delay similar or equal to the one obtained with a nonconservative analysis.

Note that the magnitude of the maximum allowable time-delay $\tau_{\max}$ in Theorem 8 is influenced by the correction gains and not by the tracking gains. In addition, for both conditions on τ resulting from (17), there exist choices for the correction gains such that it becomes possible to accommodate arbitrarily large time-delays ($k_\theta \downarrow 0$ for the first condition, and $k \downarrow 0$ for the second one, see also Fig. 5). Nonetheless, a closer examination of the proof of Theorem 8 shows that these gains also dictate the convergence rate of the predictor [refer to (27) and (30) in Appendix A]. This implies that a tradeoff exists between the magnitude of the maximum allowable time-delay and the convergence rate of the prediction error, and that this tradeoff depends on the choice of the correction gains.

C. Global Asymptotic Stability

The next theorem formulates sufficient conditions under which $(z_e^T, p_e^T)^T = 0$ is a globally uniformly asymptotically stable (GUAS) equilibrium point of (13). It is worth noting that the conditions stated in the theorem below do not explicitly place a bound on the allowable time-delay $\tau_{\max}$, but rather ensure the existence of a certain upper bound $\tau_{\max} > 0$ on the delay such that global uniform asymptotic stability can be guaranteed for any $\tau \in [0, \tau_{\max}]$. The absence of an explicit expression for $\tau_{\max}$ results in a qualitative characterization of global asymptotic stability.

Theorem 11: Consider the posture kinematic model of a unicycle robot subject to a constant input time-delay τ_f, as given by (6). The reference position of the robot is given by $(x_r(t), y_r(t))$, whereas its reference orientation $\theta_r(t)$ is given by (5a). Additionally, consider the tracking controller as given in (11), (5b), (5c), and (10). Moreover, consider the state predictor (7)–(9). Suppose that conditions A.1–A.3 and A.5 in Theorem 8 are satisfied, then, for $k_x = k_y = k > 0$ sufficiently small and $k_\theta > 0$ there exists a $\tau_{\max} > 0$ for which the equilibrium point $(z_e^T, p_e^T)^T = 0$ of the closed-loop error dynamics (13) is GUAS for all $0 \le \tau \le \tau_{\max}$.

Proof: The proof is given in Appendix B. ■

Note that, under the conditions of Theorem 11, Remarks 9 and 10 also hold for the global stability analysis.

Summarizing, we have proposed, on the one hand, a result (Theorem 8) with quantitative conditions on the time-delay that guarantee that the predictor-controller combination invokes local uniform asymptotic stability. On the other hand, we have proposed a global result (in Theorem 11), which is formulated in terms of qualitative conditions on the delays and predictor gains.

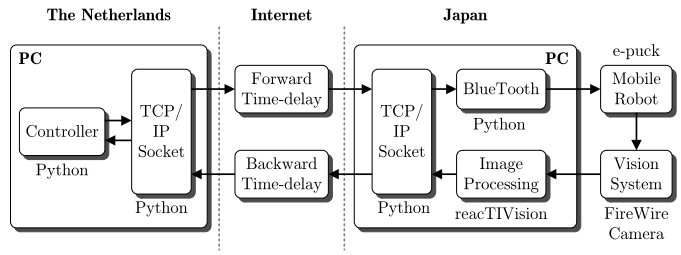

Fig. 6. Block diagram of the interconnected robotic platform.

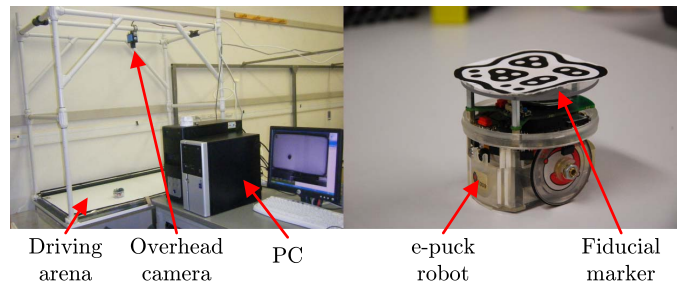

Fig. 7. Experimental setup at TMU (left) and three e-pucks equipped with unique fiducial markers (right).

V. Experimental Platform

We now introduce the robotic platform used in this paper to experimentally validate the predictor-based remote tracking control strategy proposed in Section III. The platform is available at Tokyo Metropolitan University (TMU) in Japan and connects via the Internet to a computer at the Eindhoven University of Technology (TU/e) in the Netherlands. A block diagram of the interconnected robotic platform is shown in Fig. 6. Note that the computer in Japan is used solely for communication purposes.

A. General Description

The elements of the experimental setup at TMU are briefly described in this section, for additional details we refer to [41]. The actual setup is shown on the left-hand side of Fig. 7.

1) Mobile Robot: The mobile robot used is the e-puck, shown on the right-hand side of Fig. 7, a differential-drive unicycle-type mobile robot developed at the EPFL, Switzerland [42]. The wheels of an e-puck are driven by stepper motors which receive velocity control commands over a BlueTooth connection. All the data processing required to execute these commands is carried out on the robot's onboard processor. The Python programming language is used to establish a connection with, send (control) commands to, and receive (sensor) information from the e-puck.

2) Vision System: The position and orientation of the robot is measured by static scene analysis using an industrial FireWire camera. The camera is an Imaging Source DMK-31BF03 equipped with a Computar T0412FICS-3 4-mm lens. Considering the height at which the camera is placed, the resulting size of the driving arena is of 100×50 cm. The mobile robot is fitted with a unique fiducial marker of 7×7 cm, such as the one shown on top of the robot in Fig. 7. This marker is read by reacTIVision, a standalone application which determines the position and orientation of the marker [43].

3) Sampling Rate and Bandwidth: Using the vision system results in a sampling rate of approximately 25 Hz, which constrains the bandwidth of the overall setup. Nonetheless, this choice still allows the correct polling of measurement data while ensuring an accurate control of the mobile robot.

B. Data Exchange Over the Internet

Exchanging data between the computer in the Netherlands and the experimental setup in Japan is necessary to implement the remote control strategy proposed in this paper. Because of its widespread availability and low cost, the Internet is chosen as the communication channel for this exchange.

1) Network Configuration: To establish a connection which guarantees a reliable and secure data exchange, the computer at TU/e accesses TMUs network via a virtual private network. This offers a secure access to the network without a dedicated communication channel and bypasses the difficulties posed by closed ports and other network security measures.

2) Socket Configuration: Data is transmitted as soon as it becomes available by nonblocking transmission control protocol (TCP) sockets running on of Internet protocol (IP). The low bandwidth of the system allows the use of TCP, which guarantees reliable data delivery [as opposed to user datagram protocol (UDP) sockets]. The correct serialization and deserialization of the data stream as required by Python is ensured by fixing the size of each transmitted packet and setting accordingly the reading buffer on the receiving end. As data is exchanged bidirectionally, different processing threads are set up for transmitting and receiving data.

C. Round-Trip Delay Time

The communication-induced round-trip delay time between the Netherlands and four different countries has been measured continuously during 24-h periods. Throughout this time, 2-min bursts of 1200 high-resolution ping requests have been sent to computers in Japan (http://www.jnto.go.jp), the USA (http:// www.stanford.edu), Chile (http://www.uc.cl), and Australia (http://http://www.unsw. edu.au), respectively. These bursts were repeated every 3 min, resulting in a total of 288 bursts in 24 h. The mean value of the round-trip delay for each burst is shown in Fig. 8 for all four countries, together with the 95% of the measurement. The overall mean value of the round-trip delay is around 268 ms for Japan ($3\sigma = 4.28$ ms), 178 ms for the USA ($3\sigma = 1.63$ ms), 271 ms for Chile ($3\sigma = 2.7631$ ms), and 340 ms for Australia ($3\sigma = 0.47$ ms). As could be expected from the fact that the Internet-induced delay depends on factors such as the network load, these measurements show a certain level of variability of the delay over time. Still, the delay mean (in black in Fig. 8) is remarkably constant, certainly on time scales relevant to the closed-loop dynamics of the mobile robot.

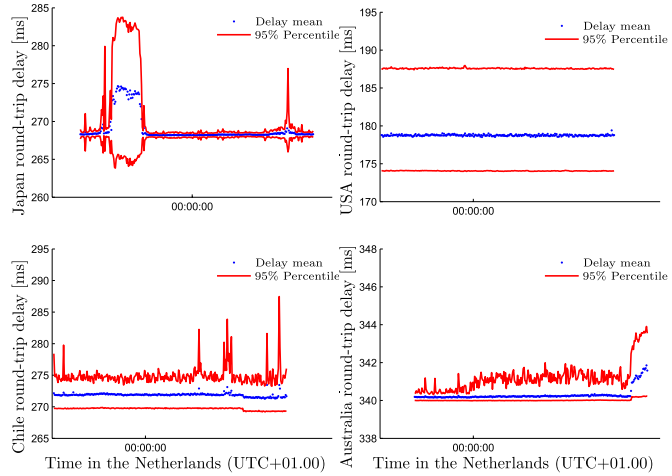

Fig. 8. 24-h round-trip delay measurement between the Netherlands and (clock-wise) Japan, the USA, Chile, and Australia.

In conclusion, the proposed network and socket configuration indeed allows a reliable data exchange with a delay which is fairly constant, especially on the time scale relevant for the tracking control of a mobile robot. In the next section, we will present experimental results in which an Internet-based communication link is used between the Netherlands and Japan to remotely control a mobile robot in Japan from a computer in the Netherlands.

VI. Simulation and Experimental Result

In this section, we present simulation and experimental results that illustrate the effectiveness and performance of the proposed remote control strategy. The remote control strategy is implemented as in Fig. 3 for all simulations and experiments. In the case of the experiments, a mobile robot at TMU is controlled from the TU/e using the interconnected robotic platform introduced in Section V. The reference trajectories for the simulations and experiments are given as follows.

1) Simulations 1–3: a circle parameterized by $(x_r(t), y_r(t)) = (x_{r_c} + r\sin\theta_r(t), y_{r_c} - r\cos\theta_r(t))$, centered at $(x_{r_c}, y_{r_c}) = (0.875, 0.65)$ [m], with

TABLE I
SIMULATION/EXPERIMENTS PARAMETERS

	Initial conditions system			Initial conditions predictor			Tracking gains			Correcting gains			Delay		
	$x(0)$ [m]	$y(0)$ [m]	$\theta(0)$ [rad]	$z_1(0)$ [m]	$z_2(0)$ [m]	$z_3(0)$ [rad]	c_x	c_y	c_θ	k_x	k_y	k_θ	τ [ms]	$\tilde{\tau}$ [ms]	$\tau_{\max}$ [ms]
Simulation 1	1.1	0.3	$\frac{\pi}{3}$	0.0	0.0	0.0	2.0	2.0	1.0	0.4	0.4	0.75	1000	1000	1100
Simulation 2	1.1	0.3	$\frac{\pi}{3}$	0.0	0.0	0.0	2.0	2.0	1.0	0.4	0.4	0.75	1000	600	1100
Simulation 3	1.1	0.3	$\frac{\pi}{3}$	0.0	0.0	0.0	2.0	2.0	1.0	0.4	0.4	0.75	1000	1400	1100
Experiment 1	0.2307	0.2191	0.2851	0.0	0.0	0.0	2.0	2.0	1.0	0.6	0.6	0.6	280	268	570
Experiment 2	0.1796	0.5975	0.3916	0.0	0.0	0.0	2.0	2.0	1.0	0.6	0.6	0.6	280	268	930

$r = 0.5$ [m], $\omega_r = 0.5$ [rad/s], and $v_r = r\omega_r = 0.25$ [m/s].

2) Experiment 1 and simulation 4: an eight curve parameterized by $(x_r(t), y_r(t)) = (x_{r_c} + a\sin(bt), y_{r_c} + c\sin(2bt))$, where $(x_{r_c}, y_{r_c}) = (0.5, 0.25)$ (m) denotes the center of the curve, $2a = 2c = 0.4$ m, its length and width, respectively, and $b = 0.2$ rad/s constitutes its angular frequency. For this reference trajectory $\bar{\omega}_r = 1.16$ rad/s.
3) Experiment 2 and simulation 5: a sinusoid parameterized by $(x_r(t), y_r(t)) = (x_{r_0} + v_{r_0}t, y_{r_0} + a\sin(\omega_{r_0}t))$, where $(x_{r_0}, y_{r_0}) = (0.1, 0.25)$ m denotes its origin, $v_{r_0} = 0.007$ m/s and $\omega_{r_0} = 0.3$ rad/s its translational and rotational velocities, respectively, and $a = 0.15$ m its amplitude. For this reference trajectory $\bar{\omega}_r = 0.48$ rad/s.

The initial conditions for the system and the state predictor, $q(0)$ and $z(0)$, respectively, are given in Table I, together with the tracking gains of the controller, the correction gains of the predictor, the actual delay τ, the estimated delay $\tilde{\tau}$ (used in the predictor-controller combination), and maximum allowable network-induced time-delay $\tau_{\max}$. Regarding the values given in Table I, recall that to satisfy the conditions in Theorem 8, the network-induced delay τ should belong to the interval $[0, \tau_{\max})$. Given the values of the maximum allowable time-delay shown in Table I [computed in accordance with condition (17) in Theorem 8, this requirement is satisfied.

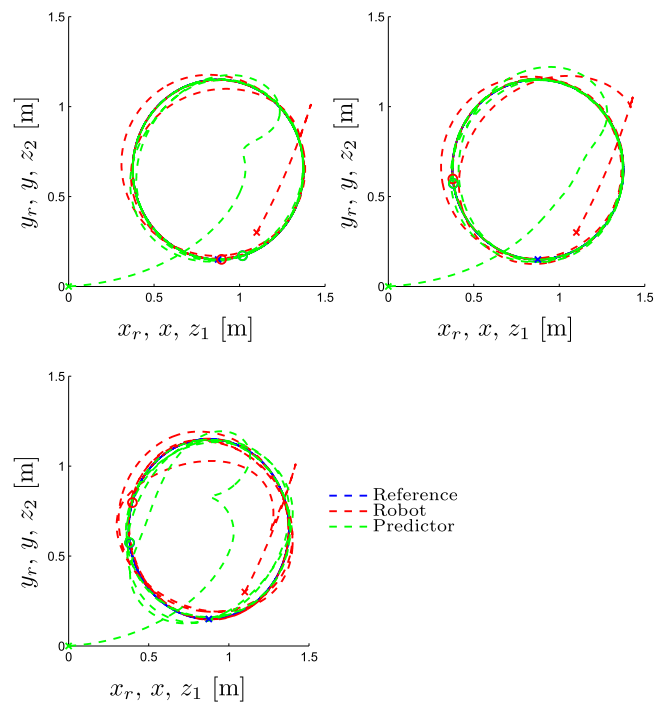

Fig. 9. Simulations of a remotely controlled unicycle with $\tau = 1000$ ms and a perturbation induced at $t = 30$ s. Top left: $\tilde{\tau} = \tau$; top right: $\tilde{\tau} = 600$ ms$< \tau$; bottom left: $\tilde{\tau} = 1400$ ms$> \tau$.

A. Simulation Result

For the first three simulations, the communication delay is taken to be $\tau = \tau_f + \tau_b = 0.5 + 0.5 = 1$ [s]. In these simulations, the delay $\tilde{\tau}$, used in the predictor-controller combination is taken to be, respectively, equal, smaller, and larger than the real delay τ (see Table I). These simulations are intended to illustrate the consequences on the remote control strategy of a large mismatch in the delay model.

The plots in Fig. 9 show the reference, robot, and predictor trajectories in the global coordinate frame $\underline{\vec{e}}^0$ for the first three simulations. The initial and final positions of these trajectories are marked with a cross and a circle, respectively. In some simulations, the reference trajectory might not be visible because of overlap with the robot and predictor trajectories. The control inputs of the robot are affected during 1.5 s, starting at $t = 30$ s, by an additive perturbation in $v(t)$ and $\omega(t)$ of 0.2 m/s and 0.3 rad/s, respectively. The purpose of perturbing the robot is to show that the proposed predictor-controller combination possesses certain robustness against perturbations.

The plots in Fig. 9 corresponding to the second and third simulations show that the remote control strategy is able to accommodate a relatively large mismatch in the delay estimate. Nevertheless, a wrong delay estimate will invariably affect the tracking performance of the system. A mismatch between the estimated delay $\tilde{\tau}$ and the actual delay τ is first reflected in the prediction error $p_e(t)$ defined in (8). As a result, the correction term (9) does not converge to zero, and the controller's output (11) is computed in terms of a predicted state $z(t)$ which does not accurately reflect the future state of the system $q(t + \tau_f)$. Consequently, the mobile robot will receive an input which is meant for an incorrectly predicted state, and a tracking error will ensue.

Further details are shown in Fig. 10. The plots in the left column show the tracking errors $e_x(t) = x_r(t - \tau_f) - x(t)$, $e_y(t) = y_r(t - \tau_f) - y(t)$, and $e_\theta(t) = \theta_r(t - \tau_f) - \theta(t)$, defined

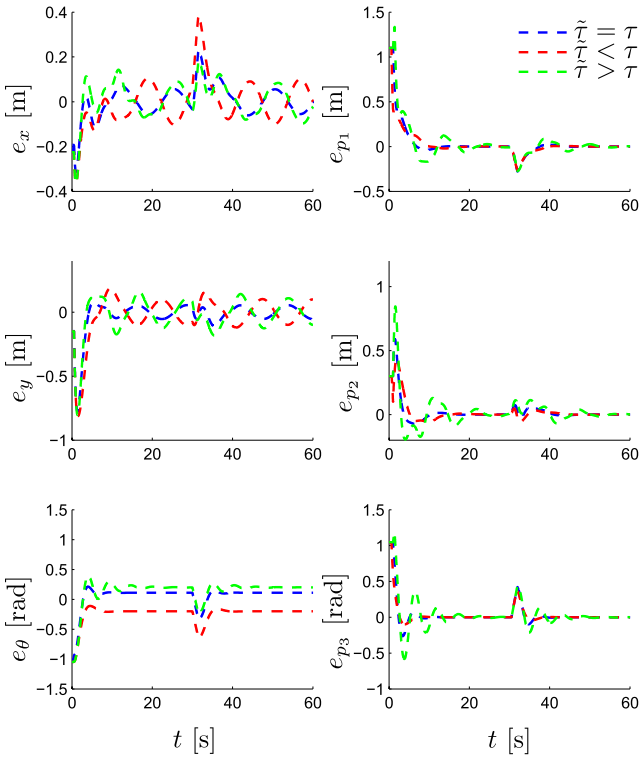

Fig. 10. Simulation results. Left column: tracking error; right column: prediction error (a perturbation is induced at $t = 30$ s).

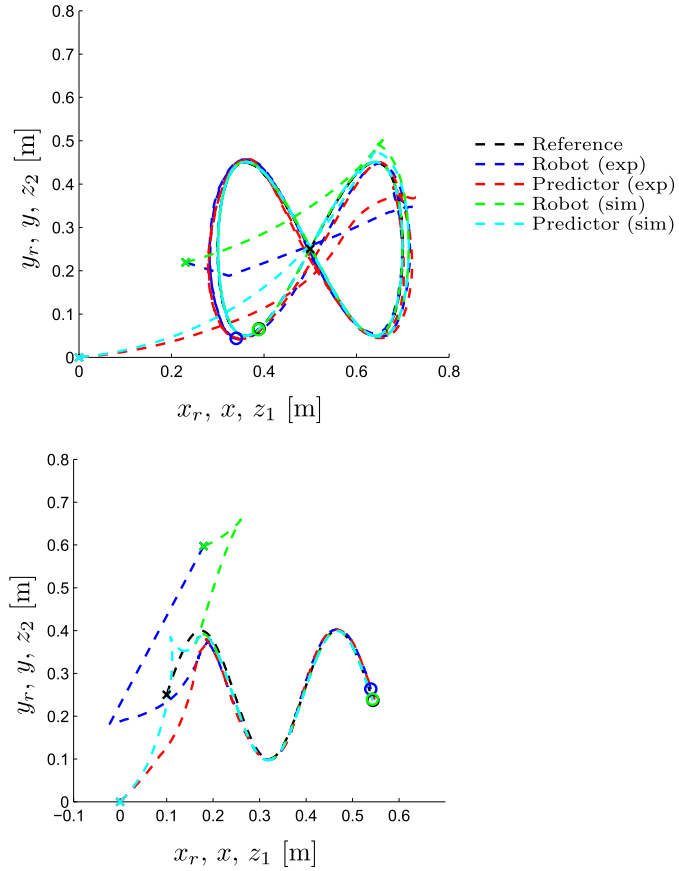

Fig. 11. Unicycle at TMU remotely controlled from TU/e. Top: first experiment. Bottom: second experiment.

in accordance with the control problem posed at the beginning of Section III-C. The plots in the right column depict the prediction errors $e_{p_1}(t) = x(t-\tau) - z_1(t-\tau)$, $e_{p_2}(t) = y(t-\tau) - z_2(t-\tau)$, and $e_{p_3}(t) = \theta(t-\tau) - z_3(t-\tau)$. As expected, all errors converge to zero when $\tilde{\tau} = \tau$ (simulation 1), whereas when $\tilde{\tau} < \tau$ and $\tilde{\tau} > \tau$ (simulations 2 and 3, respectively) the tracking performance of the mobile robot is visibly degraded, although stability (in the sense of bounded errors) is retained. In addition, the perturbation which affects the robot at $t = 30$ s is reflected on all errors and, in all cases, the remote control strategy is robust enough to overcome this disturbance.

B. Experimental Results

For the experiments, an indication for the real communication delay $\tau = 268$ ms is based on the measurements presented in Section V-C. Because of the sampling rate of the experimental platform, which is 25 Hz, only delays $\tilde{\tau}$ which are multiples of 40 ms can be implemented in software.[2] Therefore, in the experiments, the output of the predictor is delayed by $\tilde{\tau} = 280$ ms instead of $\tau = 268$ ms, with $\tilde{\tau} = \tilde{\tau}_f + \tilde{\tau}_b = \tilde{\tau}/2 + \tilde{\tau}/2$. Hence, there undoubtedly is a (small) mismatch between τ and $\tilde{\tau}$ in the experiments, which will show that the proposed remote control strategy is robust against such a mismatch.

The experimental results are accompanied by simulations with the exact same settings, except for the slightly time-varying nature of the delay in the experiments (see Section V-C). The idea is to provide a better sense of the validity of the experiments and to compare the remote control strategy for the constant delay (simulations) and time-varying delay (experiments) cases. The plots in Fig. 11 show the reference, robot, and predictor trajectories in the global coordinate frame $\underline{\vec{e}}^0$ for the experiments and their respective simulations. The initial and final positions of these trajectories are marked with a cross and a circle, respectively. The plots in the left column of Fig. 12 show the tracking errors $e_x(t), e_y(t), e_\theta(t)$, whereas the plots in the right column depict the prediction errors $e_{p_1}(t), e_{p_2}(t), e_{p_3}(t)$. Although all errors practically converge to zero and remote tracking is achieved, there is a clear difference in the settling behavior (amplitude and settling time) of the simulations and the experiments. This difference may be attributed to the small variations in the communication delay in the experiments and to other aspects of the experimental platform not considered in the simulations (dynamical effects such as wheel slip and friction, data acquisition and computational delays, sampling rate variations, the resolution of the robot's actuators, etc.). In any case, it is worth noting that for both simulations and the experiments, the time scales of the predictor and controller are clearly separated, with the one for the predictor being much faster than the one of the controller (as typically the case for an observer-controller combination).

[2]This is not an essential limitation of the proposed control strategy, but a particularity of its current implementation; it can be overcome with the application of a zero-order hold to the system's measured states.

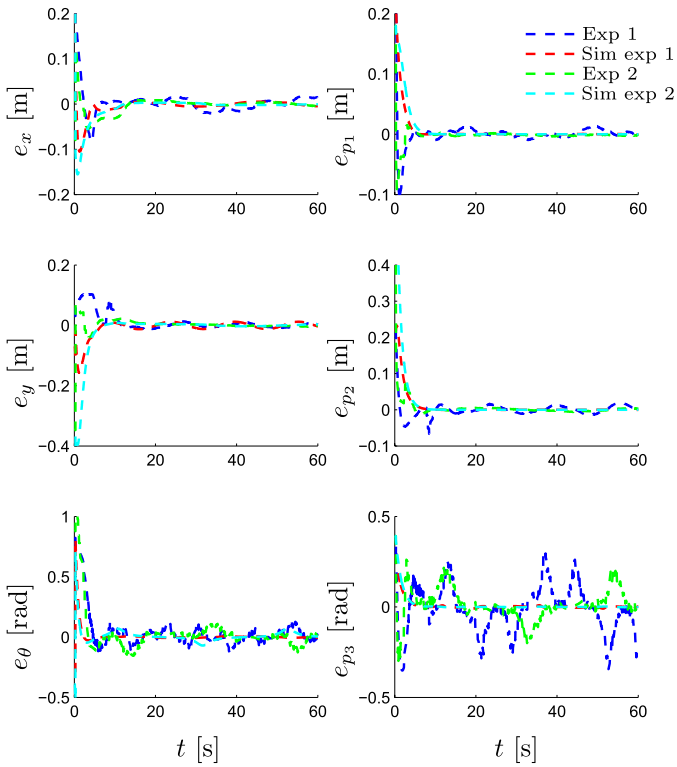

Fig. 12. Experimental results and their corresponding simulations. Left column: tracking error. Right column: prediction error.

C. Discussion

The results of the first three simulations show that the robot is able to recover from small, transient, additive perturbations. In addition, the second and third simulations demonstrate that proposed control strategy also exhibits certain robustness against large modeling errors of the time-delay. The experimental results demonstrate the fact that the tracking and prediction errors (practically) converge to zero even in the presence of a slightly time-varying time delay and a small mismatch in the delay model. The fact that $e_x(t)$, $e_y(t)$, and $e_\theta(t)$ converge to zero in the first simulation and both experiments implies that the trajectory of the robot lags the reference trajectory with a delay τ_f, in accordance with Theorem 8 and Remark 9. In conclusion, the behavior of the remote control strategy is consistent with the local stability analysis (since the conditions posed in Theorem 8 are satisfied) and the tracking performance of the robot can be ensured even in the presence of a network-induced delay.

VII. Conclusion

This paper considers the tracking control problem of a unicycle robot controlled over a two-channel communication network which induces time-delays. A tracking controller and a state predictor have been proposed which together guarantee the tracking of a delayed reference trajectory. The tracking and prediction error dynamics have been shown to be LUAS with an explicit (quantitative) upper bound on the allowable time-delay. This local stability analysis has been complemented with a global stability analysis which guarantees (qualitatively) the existence of a nonzero upper bound on the time-delay. In addition, simulations and experiments validate the effectiveness of the proposed remote control strategy and show that the predictor-controller combination can withstand small mismatches in the delay model and delay variations.

Appendix A
Proof of Theorem 8

Note that the cascaded system (13) is a particular case of the cascaded system (2) introduced in Section II. With Theorem 1, the local uniform asymptotic stability of the equilibrium point $(z_e^T, p_e^T)^T = 0$ of the closed-loop error dynamics (13) may be established if the following conditions are satisfied.

1) The system $\dot{\xi}_1(t) = A_1(t, t-\tau)\xi_1(t) + A_2\xi_1(t-\tau)$, hereinafter called the ξ_1-dynamics without coupling, is LUAS.
2) The system $\dot{\xi}_2(t) = B_1\xi_2(t) + B_2\xi_2(t-\tau)$, hereinafter called the ξ_2-dynamics, is LUAS.
3) The coupling term $g(t, \xi_{1_t}, \xi_{2_t})$ vanishes when $\xi_{2_t} \to 0$, that is, $g(t, \xi_{1_t}, 0) = 0$.

The validity of these three conditions is now checked given the requirements posed in Theorem 8.

A. Requirement on the ξ_1-Dynamics Without Coupling

Given the following state definitions: $\eta_1(t) := [z_{1_e}(t)\, z_{2_e}(t)]^T$ and $\eta_2(t) := [p_{1_e}(t)\, p_{2_e}(t)]^T$, the ξ_1-dynamics without coupling, $\dot{\xi}_1(t) = A_1(t, t-\tau)\xi_1(t) + A_2\xi_1(t-\tau)$ [taken from (13)], may be rewritten as the following cascaded system:

$$\dot{\eta}_1(t) = \Delta_1(t)\eta_1(t) + \Delta_2\eta_2(t) \tag{18a}$$
$$\dot{\eta}_2(t) = \Delta_3(t-\tau)\eta_2(t) + \Delta_4\eta_2(t-\tau) \tag{18b}$$

where

$$\Delta_1(t) = \begin{bmatrix} -c_x & (1+c_y)\omega_r(t) \\ -\omega_r(t) & 0 \end{bmatrix}$$
$$\Delta_2 = \Delta_4 = \begin{bmatrix} -k_x & 0 \\ 0 & -k_y \end{bmatrix}$$

and

$$\Delta_3(t) = \begin{bmatrix} 0 & \omega_r(t) \\ -\omega_r(t) & 0 \end{bmatrix}.$$

The local uniform asymptotic stability of the cascaded system (18) and thus of the ξ_1-dynamics without coupling can be concluded, according to Theorem 1, if the following conditions are satisfied.

1) The system $\dot{\eta}_1(t) = \Delta_1(t)\eta_1(t)$, hereinafter called the η_1-dynamics without coupling, is LUAS.
2) The system $\dot{\eta}_2(t) = \Delta_3(t-\tau)\eta_2(t) + \Delta_4\eta_2(t-\tau)$, hereinafter called the η_2-dynamics, is LUAS.
3) The coupling term $g_{\eta_1\eta_2}(t, \eta_{1_t}, \eta_{2_t}) = \Delta_2\eta_2(t)$ vanishes when $\eta_{2_t} \to 0$.

1) Requirement on the η_1-Dynamics Without Coupling: According to Lemma 1 in [40], the η_1-dynamics without coupling

$$\begin{bmatrix} \dot{z}_{1_e}(t) \\ \dot{z}_{2_e}(t) \end{bmatrix} = \begin{bmatrix} -c_x & (1+c_y)\omega_r(t) \\ -\omega_r(t) & 0 \end{bmatrix} \begin{bmatrix} z_{1_e}(t) \\ z_{2_e}(t) \end{bmatrix} \tag{19}$$

are globally exponentially stable (GES), and thus GUAS, for the requirements on c_x, c_y, and $\omega_r(t)$ posed in Theorem 8.

2) Requirement on the η_2-Dynamics: To establish the uniform asymptotic stability of the η_2-dynamics as given in (18b), let us first consider their delay-free version

$$\dot{\eta}_2(t) = \Delta_0(t)\eta_2(t) \tag{20}$$

where $\Delta_0(t) = \Delta_3(t) + \Delta_4$.

The following candidate Lyapunov function is proposed for (20):

$$V_{\eta_2} = \frac{1}{2}p_{1_e}^2 + \frac{1}{2}p_{2_e}^2 = \eta_2^T P_{\eta_2}\eta_2 \tag{21}$$

with $P_{\eta_2} = \frac{1}{2}I_2$. The time-derivative of the candidate Lyapunov function V_{η_2} is given by

$$\dot{V}_{\eta_2} = -k_x p_{1_e}^2 - k_y p_{2_e}^2 = -\eta_2^T Q_{\eta_2}\eta_2 \tag{22}$$

with

$$Q_{\eta_2} = \begin{bmatrix} k_x & 0 \\ 0 & k_y \end{bmatrix}.$$

Note that matrix P_{η_2} is positive definite, whereas matrix Q_{η_2} is positive definite for $k_x, k_y > 0$.

We will now use the Lyapunov-Razumikhin stability theorem ([34], Th. 4.2) to show that the origin of the η_2-dynamics (18b) is LUAS. Using Newton-Leibniz's law, these dynamics may be written as the following distributed delay system:

$$\begin{aligned}\dot{\eta}_2(t) = {} & \Delta_0(t-\tau)\eta_2(t) - \Delta_4\int_{t-\tau}^{t}\Delta_3(s-\tau)\eta_2(s)ds \\ & -\Delta_4^2\int_{t-\tau}^{t}\eta_2(s-\tau)ds.\end{aligned} \tag{23}$$

As the proposed Lyapunov function (21) is also a Lyapunov function for the system $\dot{\eta}_2(t) = \Delta_0(t-\tau)\eta_2(t)$ (with a decay rate characterized by the matrix Q_{η_2}), V_{η_2} will be considered as a candidate Lyapunov-Razumikhin function for the η_2-dynamics (18b). Its time-derivative, given the distributed delay system (23), satisfies

$$\begin{aligned}\dot{V}_{\eta_2} \le {} & -\eta_2^T Q_{\eta_2}\eta_2 + 2\|\eta_2\|_2\lambda_{\max}(P_{\eta_2}) \\ & \times\Bigg(\|\Delta_4\|_{i2}\sup_{t\in\mathbb{R}}\|\Delta_3(t)\|_{i2}\times\int_{-\tau}^{0}\|\eta_2(t+s)\|_2 ds \\ & + \|\Delta_4^2\|_{i2}\int_{-\tau}^{0}\|\eta_2(t+s-\tau)\|_2 ds\Bigg).\end{aligned} \tag{24}$$

The Lyapunov-Razumikhin stability theorem requires that $\dot{V}_{\eta_2}(t) < 0$ whenever

$$V_{\eta_2}(\eta_2(t+\delta)) \le pV_{\eta_2}(\eta_2(t)) \tag{25}$$

for all t and $-2\tau \le \delta \le 0$ and some $p > 1$. The condition in (25) may be rewritten in terms of $\|\eta_2(t+\delta)\|_2$ and $\|\eta_2(t)\|_2$ as follows:

$$\|\eta_2(t+\delta)\|_2 \le \sqrt{p\frac{\lambda_{\max}(P_{\eta_2})}{\lambda_{\min}(P_{\eta_2})}}\|\eta_2(t)\|_2 \tag{26}$$

for all $-2\tau \le \delta \le 0$.

Recall that the conditions in Theorem 8 state that $k := k_x = k_y$, which results in $\|\Delta_4\|_{i2} = k$ and $\|\Delta_4^2\|_{i2} = k^2$. Moreover, given $\bar{\omega}_r := \sup_{t\in\mathbb{R}}|\omega_r(t)|$, it follows that $\sup_{t\in\mathbb{R}}\|\Delta_3(t)\|_{i2} = \bar{\omega}_r$. In addition, note that $\lambda_{\max}(P_{\eta_2}) = \lambda_{\min}(P_{\eta_2}) = 1/2$ and $\lambda_{\max}(Q_{\eta_2}) = \lambda_{\min}(Q_{\eta_2}) = k$. Using these facts and condition (26), the time-derivative of the candidate Lyapunov-Razumikhin function V_{η_2} along the solutions of (18b) satisfies

$$\dot{V}_{\eta_2} \le -\big(k - \tau\sqrt{p}(k\bar{\omega}_r + k^2)\big)\|\eta_2\|_2^2. \tag{27}$$

Using the fact that $k > 0$ and $\tau < 1/\sqrt{p}(\bar{\omega}_r + k)$ [see (17)], (27) implies that $\dot{V}_{\eta_2} < 0$ under the condition (26). Hence, the η_2-dynamics are guaranteed to be LUAS.

3) Requirement on the Coupling Term $g_{\eta_1\eta_2}(t, \eta_{1_t}, \eta_{2_t})$: As the coupling term $g_{\eta_1\eta_2}(t, \eta_{1_t}, \eta_{2_t}) = \Delta_2\eta_2(t)$, we obviously have that $g_{\eta_1\eta_2}(t, \eta_{1_t}, \eta_{2_t}) \to 0$ as $\eta_{2_t} \to 0$.

B. Requirement on the ξ_2-Dynamics

The ξ_2-dynamics in (13b) may be rewritten as the following cascaded system:

$$\dot{z}_{3_e}(t) = -c_\theta z_{3_e}(t) - k_\theta p_{3_e}(t) \tag{28a}$$

$$\dot{p}_{3_e}(t) = -k_\theta p_{3_e}(t-\tau). \tag{28b}$$

To deduce the local uniform asymptotic stability of the cascaded system (28) using Theorem 1 [and thus of the ξ_2-dynamics (13b)], the following conditions should be satisfied.

1) The system $\dot{z}_{3_e}(t) = -c_\theta z_{3_e}(t)$, denoted hereinafter as the z_{3_e}-dynamics without coupling is LUAS, which is ensured for $c_\theta > 0$.
2) The system $\dot{p}_{3_e}(t) = -k_\theta p_{3_e}(t-\tau)$ in (28b) is LUAS. Namely, given the characteristic quasi-polynomial of (28b)

$$s + k_\theta e^{-s\tau} = 0 \tag{29}$$

the uniform asymptotic stability of the p_{3_e}-dynamics is ensured for

$$\tau < \frac{\pi}{2k_\theta} \tag{30}$$

with $k_\theta > 0$ [which is satisfied due to (17)].
3) The coupling term $g_{z_3p_3}(t, z_{3_t}, p_{3_t}) = -k_\theta p_{3_e}(t)$ vanishes as $p_{3_t} \to 0$, which is clearly the case.

C. Requirement on the Coupling Term $g(t, \xi_{1_t}, \xi_{2_t})$

The coupling term $g(t, \xi_{1_t}, \xi_{2_t})$ clearly vanishes as $\xi_{2_t} \to 0$.

In conclusion, the local uniform asymptotic stability of the equilibrium point $(z_e^T, p_e^T)^T = 0$ of the closed-loop error dynamics (13) may be established provided that the conditions in Theorem 8 are met. This completes the proof.

APPENDIX B
PROOF OF THEOREM 11

With Theorem 2, the following conditions may be posed to establish the global uniform asymptotic stability of the equilibrium point $(z_e^T, p_e^T)^T = 0$ of the closed-loop error dynamics represented by the cascaded system (13):

1) the ξ_1-dynamics without coupling are GES with a quadratic Lyapunov-Razumikhin function V_{ξ_1};

2) the ξ_2-dynamics are GES;
3) the coupling term $g(t, \xi_{1_t}, \xi_{2_t})$ admits the estimate

$$\|g(t, \varphi_{\xi_1}, \varphi_{\xi_2})\|_1 \leq (\alpha_1(\|\varphi_{\xi_2}\|_c) + \alpha_2(\|\varphi_{\xi_2}\|_c)\|\varphi_{\xi_1}\|_c)\|\varphi_{\xi_2}\|_c \tag{31}$$

for continuous functions $\alpha_1, \alpha_2 : \mathbb{R}^+ \to \mathbb{R}^+$.

The global exponential stability requirements on the ξ_1-dynamics without coupling and the ξ_2-dynamics are based on the assumptions in Theorem 2 and Remark 3. In the case of the ξ_1-dynamics without coupling, the first four assumptions in Theorem 2 are satisfied if the global uniform asymptotic stability of the system is characterized by a strict Lyapunov-Razumikhin function, and the fifth assumption is fulfilled if the associated Lyapunov-Razumikhin function is quadratic. It then follows that requiring the ξ_1-dynamics to be GES with a quadratic strict Lyapunov-Razumikhin function will satisfy all the assumptions in Theorem 2 (one to five) related to them. Regarding the ξ_2-dynamics, the seventh assumption in Theorem 2 poses the requirement for the global exponential stability of these dynamics. It is also worth noting that, because of the stability requirement on the ξ_1-dynamics without coupling, the estimate on the coupling term may be rewritten as in (31) according to Remark 3.

The validity of the previous three conditions will now be checked given the requirements posed in Theorem 11.

A. Requirement on the ξ_1-Dynamics Without Coupling

Recall that given the state definitions: $\eta_1(t) := [z_{1_e}(t)\, z_{2_e}(t)]^T$ and $\eta_2(t) := [p_{1_e}(t)\; p_{2_e}(t)]^T$, the ξ_1-dynamics without coupling, $\dot{\xi}_1(t) = A_1(t, t-\tau)\xi_1(t) + A_2\xi_1(t-\tau)$, may be rewritten as in (18). For zero delay ($\tau = 0$), this cascaded system is given by the following linear time-varying system:

$$\dot{\eta}_1(t) = \Delta_1(t)\eta_1(t) + \Delta_2\eta_2(t) \tag{32a}$$

$$\dot{\eta}_2(t) = (\Delta_3(t) + \Delta_4)\eta_2(t). \tag{32b}$$

The delay-free η_1-dynamics without coupling in (32a) are given as in (19), and have already been shown to be GES in the proof of Theorem 8. From Lyapunov converse theory we know that, since the delay-free η_1-dynamics without coupling are GES, there exists, for all t, a continuously differentiable, bounded, positive definite, symmetric matrix $P_{\eta_1}(t)$ that satisfies

$$-\dot{P}_{\eta_1}(t) = P_{\eta_1}(t)\Delta_1(t) + \Delta_1^T(t)P_{\eta_1}(t) + Q_{\eta_1}(t) \quad \forall t \tag{33}$$

where $Q_{\eta_1}(t)$ is continuous, bounded, positive definite, and symmetric, and $\Delta_1(t)$ is required to be continuous in t and bounded for all t. The requirement on $\Delta_1(t)$ is satisfied since $\omega_r(t)$ is continuous and bounded, as it is persistently exciting (see Def. 4). As a result, $V_{\eta_1} = \eta_1^T P_{\eta_1}(t)\eta_1$ is a Lyapunov function for the delay-free η_1-dynamics without coupling. The derivative of this function satisfies

$$\dot{V}_{\eta_1} = -\eta_1^T Q_{\eta_1}(t)\eta_1 \leq -\beta_1\|\eta_1\|_2^2 \tag{34}$$

where $\beta_1 := \inf_{t\in\mathbb{R}} \lambda_{\min}(Q_{\eta_1}(t))$.

On the other hand, the delay-free η_2-dynamics (32b) have already been shown to be GES for $k_x, k_y > 0$ in the proof of Theorem 8, with the Lyapunov function V_{η_2} defined in (21).

We now propose

$$V_{\xi_1} = V_{\eta_1} + V_{\eta_2} = \eta_1^T P_{\eta_1}(t)\eta_1 + \eta_2^T P_{\eta_2}\eta_2 \tag{35}$$

as a candidate Lyapunov-Razumikhin function for the ξ_1-dynamics without coupling, use the Lyapunov-Razumikhin stability theorem to show that the origin of these error dynamics is GES and that (35) is a Lyapunov-Razumkhin function which satisfies the requirements stated in Theorem 11.

Recall that by using Newton-Leibniz's law, the η_2-dynamics (18b) may be written as the distributed delay system (23). Considering this, the time-derivative of the candidate Lyapunov-Razumikhin function (35) is given by

$$\begin{aligned}\dot{V}_{\xi_1} \leq & -\beta_1\|\eta_1\|_2^2 + 2\sup_{t\in\mathbb{R}}(\|P_{\eta_1}(t)\|_{i2})\|\Delta_2\|_{i2}\|\eta_1\|_2\|\eta_2\|_2 \\ & - \eta_2^T Q_{\eta_2}\eta_2 + 2\|\eta_2\|_2\lambda_{\max}(P_{\eta_2}) \\ & \times \Bigg(\|\Delta_4\|_{i2}\sup_{t\in\mathbb{R}}\|\Delta_3(t)\|_{i2}\int_{-\tau}^{0}\|\eta_2(t+s)\|_2 ds \\ & + \|\Delta_4^2\|_{i2}\int_{-\tau}^{0}\|\eta_2(t+s-\tau)\|_2 ds\Bigg).\end{aligned} \tag{36}$$

The Lyapunov-Razumikhin stability theorem requires that $\dot{V}_{\xi_1}(t) < 0$ whenever

$$V_{\xi_1}(\xi_1(t+\delta)) \leq pV_{\xi_1}(\xi_1(t)) \tag{37}$$

for all t and $-2\tau \leq \delta \leq 0$ and some $p > 1$. The condition in (37) may be rewritten in terms of V_{η_1} and V_{η_2} as

$$\begin{aligned}V_{\eta_1}(\eta_1(t+\delta)) + V_{\eta_2}(\eta_2(t+\delta)) \\ \leq p\left(V_{\eta_1}(\eta_1(t)) + V_{\eta_2}(\eta_2(t))\right)\end{aligned} \tag{38}$$

for all t and $-2\tau \leq \delta \leq 0$ and some $p > 1$. It is possible to replace condition (38) by a condition given in terms of $\|\eta_1(t+\delta)\|_2$, $\|\eta_1(t)\|_2$, $\|\eta_2(t+\delta)\|_2$, and $\|\eta_2(t)\|_2$ as follows:

$$\begin{aligned}\|\eta_2(t+\delta)\|_2 \leq \Bigg(p\frac{\sup_{t\in\mathbb{R}}\left(\lambda_{\max}(P_{\eta_1}(t))\right)}{\lambda_{\min}(P_{\eta_2})}\|\eta_1(t)\|_2^2 \\ + p\frac{\lambda_{\max}(P_{\eta_2})}{\lambda_{\min}(P_{\eta_2})}\|\eta_2(t)\|_2^2\Bigg)^{1/2}.\end{aligned} \tag{39}$$

With $\|a\|_2 \leq \|a\|_1$, (39) may be replaced by the following condition:

$$\begin{aligned}\|\eta_2(t+\delta)\|_2 \leq \sqrt{p\frac{\sup_{t\in\mathbb{R}}\left(\lambda_{\max}(P_{\eta_1}(t))\right)}{\lambda_{\min}(P_{\eta_2})}}\|\eta_1(t)\|_2 \\ + \sqrt{p\frac{\lambda_{\max}(P_{\eta_2})}{\lambda_{\min}(P_{\eta_2})}}\|\eta_2(t)\|_2.\end{aligned} \tag{40}$$

Given (36) and using condition (40), the time-derivative of the candidate Lyapunov-Razumikhin function V_{ξ_1} satisfies

$$\dot{V}_{\xi_1} \leq -\beta_1\|\eta_1\|_2^2 - \beta_2\|\eta_2\|_2^2 + \beta_3\|\eta_1\|_2\|\eta_2\|_2 \tag{41}$$

where

$$\beta_2 := \beta_{21} + \beta_{22}\tau \tag{42a}$$

$$\beta_3 := \beta_{31} + \beta_{32}\tau \tag{42b}$$

with

$$\begin{aligned}\beta_{21} &= \lambda_{\min}(Q_{\eta_2})\\ \beta_{22} &= -2\lambda_{\max}(P_{\eta_2})\sqrt{p\frac{\lambda_{\max}(P_{\eta_2})}{\lambda_{\min}(P_{\eta_2})}}\\ &\quad\times\left(\|\Delta_4\|_{i2}\sup_{t\in\mathbb{R}}\|\Delta_3(t)\|_{i2}+\|\Delta_4^2\|_{i2}\right)\\ \beta_{31} &= 2\sup_{t\in\mathbb{R}}(\|P_{\eta_1}(t)\|_{i2})\|\Delta_2\|_{i2}\\ \beta_{32} &= 2\lambda_{\max}(P_{\eta_2})\sqrt{p\frac{\sup_{t\in\mathbb{R}}\left(\lambda_{\max}(P_{\eta_1}(t))\right)}{\lambda_{\min}(P_{\eta_2})}}\\ &\quad\times\left(\|\Delta_4\|_{i2}\sup_{t\in\mathbb{R}}\|\Delta_3(t)\|_{i2}+\|\Delta_4^2\|_{i2}\right).\end{aligned}\tag{43}$$

Considering that for all $\gamma > 0$ it holds that $\|\eta_1\|_2\|\eta_2\|_2 \leq \gamma\|\eta_1\|_2^2 + \frac{1}{\gamma}\|\eta_2\|_2^2$, (41) may be rewritten as follows:

$$\begin{aligned}\dot{V}_{\xi_1} \leq &-(\beta_1-(\beta_{31}+\beta_{32}\tau)\gamma)\|\eta_1\|_2^2\\ &-\left((\beta_{21}+\beta_{22}\tau)-(\beta_{31}+\beta_{32}\tau)\frac{1}{\gamma}\right)\|\eta_2\|_2^2.\end{aligned}\tag{44}$$

Recall that the conditions in Theorem 11 state that $k := k_x = k_y$, so we have that $\|\Delta_2\|_{i2} = \|\Delta_4\|_{i2} = k$ and $\|\Delta_4^2\|_{i2} = k^2$. Moreover, given $\bar{\omega}_r := \sup_{t\in\mathbb{R}}|\omega_r(t)|$, it follows that $\sup_{t\in\mathbb{R}}\|\Delta_3(t)\|_{i2} = \bar{\omega}_r$. In addition, note that $\lambda_{\max}(P_{\eta_2}) = \lambda_{\min}(P_{\eta_2}) = \frac{1}{2}$ and $\lambda_{\max}(Q_{\eta_2}) = \lambda_{\min}(Q_{\eta_2}) = k$. Considering these facts, β_2 and β_3, as defined in (42a) and (42b), respectively, may be rewritten as

$$\beta_2 = \underbrace{k}_{\beta_{21}}\underbrace{-\sqrt{p}k(\bar{\omega}_r+k)}_{\beta_{22}}\tau \tag{45a}$$

$$\beta_3 = \underbrace{2k\sup_{t\in\mathbb{R}}\|P_{\eta_1}(t)\|_{i2}}_{\beta_{31}}\underbrace{+k(\bar{\omega}_r+k)\sqrt{2p\sup_{t\in\mathbb{R}}\|P_{\eta_1}(t)\|_{i2}}}_{\beta_{32}}\tau. \tag{45b}$$

From (44) and the definitions in (45), we conclude that it is possible to pose requirements on the tracking gains c_x, c_y, c_θ, correction gains k_x, k_y, k_θ, reference rotational velocity $\omega_r(t)$, and allowable time-delay such that the condition for global exponential stability of the ξ_1-dynamics without coupling is met. Posing these requirements in terms of the time-delay τ yields

$$\tau < \frac{\beta_1-\gamma\beta_{31}}{\beta_{32}\gamma} \tag{46}$$

and

$$\tau < \frac{\beta_{21}\gamma-\beta_{31}}{\beta_{32}-\beta_{22}\gamma} \tag{47}$$

which may be rewritten as follows by taking (45a) and (45b) into account:

$$\tau < \frac{\inf_{t\in\mathbb{R}}\lambda_{\min}(Q_{\eta_1}(t)) - 2\gamma k\sup_{t\in\mathbb{R}}\|P_{\eta_1}(t)\|_{i2}}{\gamma k(\bar{\omega}_r+k)\sqrt{2p\sup_{t\in\mathbb{R}}\|P_{\eta_1}(t)\|_{i2}}} \tag{48}$$

and

$$\tau < \frac{\gamma-2\sup_{t\in\mathbb{R}}\|P_{\eta_1}(t)\|_{i2}}{(\bar{\omega}_r+k)(\gamma\sqrt{p}+\sqrt{2p\sup_{t\in\mathbb{R}}\|P_{\eta_1}(t)\|_{i2}})}. \tag{49}$$

Given the fact that $\sup_{t\in\mathbb{R}}\|P_{\eta_1}(t)\|_{i2}$ is bounded and $\inf_{t\in\mathbb{R}}\lambda_{\min}(Q_{\eta_1}(t)) > 0$, the previous conditions imply that there exist $k > 0$ sufficiently small and $\gamma > 0$ sufficiently large so that there exists $\tau_{\max} > 0$ such that (48) and (49) are satisfied for all $\tau \in [0, \tau_{\max}]$. Hence, for all $0 \leq \tau \leq \tau_{\max}$, there exist $k > 0$ sufficiently small and $\gamma > 0$ sufficiently large for which $\xi_1 = 0$ is a GES equilibrium point of the ξ_1-dynamics without coupling. In this sense, we pose two conditions that can always be fulfilled. Namely, first choose γ large enough to satisfy condition (49). Then, choose k small enough to satisfy condition (48). Note that as $\gamma \to \infty$, it is necessary for $k \downarrow 0$. Considering the previous remarks, it is possible to conclude that $k > 0$ can always be chosen small enough such that the ξ_1-dynamics without coupling are GES.

B. Requirement on the ξ_2-Dynamics

Recall that the (local) uniform asymptotic stability of these dynamics has already been established in the proof of Theorem 8. As the system is linear time-invariant, the global exponential stability of the system immediately follows provided that c_θ and k_θ satisfy the conditions in Theorem 11 and:

$$\tau < \frac{\pi}{2k_\theta}. \tag{50}$$

C. Requirement on the Coupling Term $g(t, \xi_{1_t}, \xi_{2_t})$

We are required to show that there exist continuous functions $\alpha_1, \alpha_2 : \mathbb{R}^+ \to \mathbb{R}^+$ such that the coupling term admits the estimate (31). To begin with, the coupling term is rewritten in terms of φ_{ξ_1} and φ_{ξ_2} as follows:

$$\begin{aligned}g(t,\varphi_{\xi_1},\varphi_{\xi_2}) = &\ g_1(t,t-\tau,\varphi_{\xi_1},\varphi_{\xi_2}(0))\xi_2(t)\\ &+g_2(\varphi_{\xi_1}(0))\xi_2(t-\tau)\end{aligned}\tag{51}$$

with

$$g_1(t,t-\tau,\varphi_{\xi_1},\varphi_{\xi_2}(0)) = \begin{bmatrix} g_{11} & k_\theta z_{2_e}(t)\\ g_{21} & -k_\theta z_{1_e}(t)\\ 0 & g_{32}\\ 0 & g_{42}\end{bmatrix}$$

$$g_2(\varphi_{\xi_1}(0)) = \begin{bmatrix} 0 & 0\\ 0 & 0\\ c_\theta p_{2_e}(t) & k_\theta p_{2_e}(t)\\ -c_\theta p_{1_e}(t) & -k_\theta p_{1_e}(t)\end{bmatrix}$$

and g_{11}, g_{21}, g_{32}, and g_{42} have already been defined in (15).

Considering (51) and the fact that $\|A\|_{i1} \leq \|A\|_{\text{sum}}$, the following holds:

$$\begin{aligned}&\|g(t,\varphi_{\xi_1},\varphi_{\xi_2})\|_1\\ &= \|g_1(t,t-\tau,\varphi_{\xi_1},\varphi_{\xi_2}(0))\varphi_{\xi_2}(0)+g_2(\varphi_{\xi_1}(0))\varphi_{\xi_2}(-\tau)\|_1\\ &\leq \left(\|g_1(t,t-\tau,\varphi_{\xi_1},\varphi_{\xi_2}(0))\|_{\text{sum}}+\|g_2(\varphi_{\xi_1}(0))\|_{\text{sum}}\right)\|\varphi_{\xi_2}\|_c.\end{aligned}\tag{52}$$

It then follows that, in order to satisfy the requirement on the coupling term, it suffices to show that there exist continuous functions $\alpha_1, \alpha_2 : \mathbb{R}^+ \to \mathbb{R}^+$ such that the following inequality is satisfied:

$$\begin{aligned}&\|g_1(t,t-\tau,\varphi_{\xi_1},\varphi_{\xi_2}(0))\|_{\text{sum}}+\|g_2(\varphi_{\xi_1}(0))\|_{\text{sum}}\\ &\qquad\leq \alpha_1(\|\varphi_{\xi_2}\|_c)+\alpha_2(\|\varphi_{\xi_2}\|_c)\|\varphi_{\xi_1}\|_c.\end{aligned}\tag{53}$$

Considering the coupling term expressed in terms of particular solutions of (13), the definition of the sum matrix norm, the triangle inequality, and the equalities defined in (16) (which are continuous and always ≤ 1 for all x), the following condition results from (53):

$$\begin{aligned}\|g_1(t,t-\tau,\xi_{1_t},\xi_{2_t}(0))\|_{\text{sum}} &+ \|g_2(\xi_{1_t}(0))\|_{\text{sum}} \\ &\leq \big(|c_\theta|+|k_\theta|\big)\big(|z_{1_e}(t)|+|z_{2_e}(t)|+|p_{1_e}(t)| \\ &\quad + |p_{2_e}(t)|\big)+2|v_r(t)| + 2|v_r(t-\tau)| \\ &\quad + 2|c_x z_{1_e}(t-\tau)|+2|c_y\omega_r(t-\tau)z_{2_e}(t-\tau)|. \qquad (54)\end{aligned}$$

Recall that the theorem requires $c_x, c_\theta, k_\theta > 0, c_y > -1$, and $\bar{\omega}_r = \sup_{t\in\mathbb{R}} |\omega_r(t)|$. In addition, as $v_r(t)$ is bounded, we may define $\bar{v}_r := \sup_{t\in\mathbb{R}} |v_r(t)|$. Inequality (54) now yields

$$\begin{aligned}\|g_1(t,t-\tau,\xi_{1_t},\xi_{2_t}(0))\|_{\text{sum}} &+ \|g_2(\xi_{1_t}(0))\|_{\text{sum}} \\ &\leq (c_\theta+k_\theta)\left(\left|z_{1_e}(t)\right|+\left|z_{2_e}(t)\right|+\left|p_{1_e}(t)\right|+\left|p_{2_e}(t)\right|\right) \\ &\quad + 4\,|\bar{v}_r| + 2c_x\left|z_{1_e}(t-\tau)\right|+2|c_y|\bar{\omega}_r\left|z_{2_e}(t-\tau)\right| \\ &\leq 4\,|\bar{v}_r|+(c_\theta+k_\theta+2(c_x+|c_y|\bar{\omega}_r))\|\xi_{1_t}\|_c. \qquad (55)\end{aligned}$$

Expressing inequality (55) in terms of φ_{ξ_1} and φ_{ξ_2} (i.e., for any elements of the Banach spaces $\mathcal{C}(4)$ and $\mathcal{C}(2)$, respectively) results in

$$\begin{aligned}\|g_1(t,t-\tau,\varphi_{\xi_1},\varphi_{\xi_2}(0))\|_{\text{sum}} &+ \|g_2(\varphi_{\xi_1}(0))\|_{\text{sum}} \\ &\leq 4\,|\bar{v}_r|+(c_\theta+k_\theta+2(c_x+|c_y|\bar{\omega}_r))\|\varphi_{\xi_1}\|_c. \qquad (56)\end{aligned}$$

From (56) we have that inequality (53) is satisfied for $\alpha_1(\|\varphi_{\xi_2}\|_c) = 4|\bar{v}_r|$ and $\alpha_2(\|\varphi_{\xi_2}\|_c) = 4(c_\theta + k_\theta + 2(c_x + |c_y|\bar{\omega}_r))$. This means that the requirement on the coupling term is met.

After checking the three conditions formulated at the beginning of the proof, the global uniform asymptotic stability of the equilibrium point $(z_e^T, p_e^T)^T = 0$ of the closed-loop error dynamics (13) can be concluded, provided that the conditions in Theorem 11 for the control parameters are met. These conditions imply that there exist correction gains $k = k_x = k_y > 0$ sufficiently small, $k_\theta > 0$, and a constant $\gamma > 0$ sufficiently large such that the conditions on τ posed in (48)–(50) are satisfied, and for which the origin of the closed-loop error dynamics (13). This completes the proof.

REFERENCES

[1] L. Whitcomb, "Underwater robotics: Out of the research laboratory and into the field," in *Proc. IEEE Int. Conf. Robot. Autom.*, San Franciso, CA, USA, Apr. 2000, pp. 709–716.

[2] J. Biesiadecki, E. Baumgartner, R. Bonitz, B. Cooper, F. Hartman, P. Leger, *et al.*, "Mars exploration rover surface operations: Driving opportunity at meridiani planum," *IEEE Robot. Autom. Mag.*, vol. 13, no. 2, pp. 63–71, Jun. 2006.

[3] Y. Ho, H. Masuda, H. Oda, and L. Stark, "Distributed control for teleoperations," *IEEE/ASME Trans. Mechatron.*, vol. 5, no. 2, pp. 100–109, Jun. 2000.

[4] N. Vagenas, H. Sjoberg, and S. Wokstrom, "Application of remote-controlled/automatic load-haul-dump system in Zinkgruvan, Sweden," in *Proc. 1st Int. Symp. Mine Mech. Autom.*, Golden, CO, USA, 1991, pp. 1–2.

[5] R. Murphy, "Trial by fire [rescue robots]," *IEEE Robot. Autom. Mag.*, vol. 11, no. 3, pp. 50–61, Sep. 2004.

[6] S. Sanders, "Remote operations for fusion using teleoperation," *Ind. Robot., An Int. J.*, vol. 33, no. 3, pp. 174–177, 2006.

[7] P. Hokayem and M. Spong, "Bilateral teleoperation: An historical survey," *Automatica*, vol. 42, no. 12, pp. 2035–2057, 2006.

[8] B. Siciliano and O. Khatib, *Springer Handbook of Robotics*. Berlin, Germany: Springer-Verlag, 2008.

[9] K. Hashtrudi-Zaad and S. Salcudean, "Transparency in time-delayed systems and the effect of local force feedback for transparent teleoperation," *IEEE Trans. Robot. Autom.*, vol. 18, no. 1, pp. 108–114, Feb. 2002.

[10] W. Kim, B. Hannaford, and A. Bejczy, "Force reflection and shared compliant control in operating telemanipulators with time delays," *IEEE Trans. Robot. Autom.*, vol. 8, no. 2, pp. 176–185, Apr. 1992.

[11] S. Stramigioli, A. van der Schaft, B. Maschke, and C. Melchiorri, "Geometric scattering in robotic telemanipulation," *IEEE Trans. Robot. Autom.*, vol. 18, no. 4, pp. 588–596, Aug. 2002.

[12] B. Hannaford and J.-H. Ryu, "Time domain passivity control of haptic interfaces," *IEEE Trans. Robot. Autom.*, vol. 18, no. 1, pp. 1–10, Feb. 2002.

[13] G. Niemeyer and J.-J. Slotine, "Telemanipulation with time delays," *Int. J. Robot. Res.*, vol. 23, no. 9, pp. 873–890, 2004.

[14] D. Lee, O. Martinez-Palafox, and M. Spong, "Bilateral teleoperation of mobile robot over delayed communication network," in *Proc. IEEE Int. Conf. Robot. Autom.*, Orlando, FL, USA, May 2006, pp. 3298–3303.

[15] N. Leonard, D. Paley, F. Lekien, R. Sepulchre, D. Fratantoni, and R. Davis, "Collective motion, sensor networks, and ocean sampling," *Proc. IEEE*, vol. 95, no. 1, pp. 48–74, Jan. 2007.

[16] J. Hespanha, P. Naghshtabrizi, and Y. Xu, "A survey of recent results in networked control systems," *Proc. IEEE*, vol. 95, no. 1, pp. 138–162, Jan. 2007.

[17] D. Nešić and D. Liberzon, "A unified framework for design and analysis of networked and quantized control systems," *IEEE Trans. Autom. Control*, vol. 54, no. 4, pp. 732–747, Apr. 2009.

[18] W. Heemels, A. Teel, N. van de Wouw, and D. Nešić, "Networked control systems with communication constraints: Tradeoffs between transmission intervals, delays and performance," *IEEE Trans. Autom. Control*, vol. 55, no. 8, pp. 1781–1796, Aug. 2010.

[19] N. van de Wouw, P. Naghshtabrizi, M. Cloosterman, and J. Hespanha, "Tracking control for sampled-data systems with uncertain sampling intervals and delays," *Int. J. Robust Nonlinear Control*, vol. 20, no. 4, pp. 387–411, 2010.

[20] H. Gao, T. Chen, and J. Lam, "A new delay system approach to network-based control," *Automatica*, vol. 44, no. 1, pp. 39–52, 2008.

[21] R. Postoyan, N. van de Wouw, D. Nešić, and W. Heemels, "Emulation-based tracking solutions for nonlinear networked control systems," in *Proc. 51st IEEE CDC*, Maui, HI, USA, Dec. 2012, pp. 740–745.

[22] H. Voss, "Anticipating chaotic synchronization," *Phys. Rev. E*, vol. 61, no. 15, pp. 5115–5119, 2000.

[23] T. Oguchi and H. Nijmeijer, "Anticipating synchronization of nonlinear systems with uncertainties," in *Proc. 6th IFAC Workshop Time-Delay Syst.*, L'Aquila, Italy, 2006, pp. 290—295.

[24] T. Oguchi and H. Nijmeijer, "Control of nonlinear systems with time-delay using state prediction based on synchronization," in *Proc. ENOC*, Eindhoven, The Netherlands, 2005, pp. 1150–1156.

[25] O. Smith, "Closer control of loops with dead time," *Chem. Eng. Progr.*, vol. 53, no. 5, pp. 217–219, 1957.

[26] C. Kravaris and R. Wright, "Deadtime compensation for nonlinear processes," *AIChE J.*, vol. 35, no. 9, pp. 1535–1542, 1989.

[27] M. Henson and D. Seborg, "Time-delay compensation for nonlinear processes," *Ind. Eng. Chem. Res.*, vol. 33, no. 6, pp. 1493–1500, 1994.

[28] J. Normey-Rico and E. Camacho, "Dead-time compensators: A survey," *Control Eng. Practice*, vol. 16, no. 4, pp. 407–428, 2008.

[29] A. Smith and K. Hashtrudi-Zaad, "Smith predictor type control architectures for time delayed teleoperation," *Int. J. Robot. Res.*, vol. 25, no. 8, pp. 797–818, 2006.

[30] I. Karafyllis and M. Krstic, "Nonlinear stabilization under sampled and delayed measurements, and with inputs subject to delay and zero-order hold," *IEEE Trans. Autom. Control*, vol. 57, no. 5, pp. 1141–1154, May 2012.

[31] M. Krstic, *Delay Compensation for Nonlinear, Adaptive, and PDE Systems* (ser. Systems & Control: Foundations & Applications). Boston, MA, USA: Birkhäuser, 2009.

[32] A. Alvarez-Aguirre, H. Nijmeijer, N. van de Wouw, T. Oguchi, and K. Kojima, *Informatics in Control, Automation and Robotics* (ser. Lecture Notes in Electrical Engineering Series (LNEE)). Berlin, Germany: Springer-Verlag, 2011, pp. 225–238.

[33] K. Gu, V. Kharitonov, and J. Chien, *Stability of Time-Delay Systems*. Boston, MA, USA: Birkhäuser, 2003.

[34] J. Hale and S. Verduyn-Lunel, *Introduction to Functional Differential Equations*. Berlin, Germany: Springer-Verlag, 1993.

[35] N. Sedova, "Local and semiglobal stabilization in a cascade with delays," *Autom. Remote Control*, vol. 69, no. 6, pp. 968–979, 2008.

[36] N. Sedova, "The global asymptotic stability and stabilization in nonlinear cascade systems with delay," *Russian Math.*, vol. 52, no. 22, pp. 68–79, 2008.

[37] E. Lefeber, "Tracking control of nonlinear mechanical systems," Ph.D. dissertation, Dept. Comput. Sci., Univ. Twente, Enschede, The Netherlands, 2000,

[38] B. Siciliano, L. Sciavicco, L. Villani, and G. Oriolo, *Robotics: Modelling, Planning and Control*. New York, NY, USA: Springer-Verlag, 2009.

[39] W. Michiels and S.-I. Niculescu, *Stability and Stabilization of Time-Delay Systems: An Eigenvalue-Based Approach* (ser. Advances in Design and Control). Philadelphia, PA, USA: SIAM, 2007.

[40] J. Jakubiak, E. Lefeber, K. Tchoń, and H. Nijmeijer, "Two observer-based tracking algorithms for a unicycle mobile robot," *Int. J. Appl. Math. Comput. Sci.*, vol. 12, no. 4, pp. 513–522, 2002.

[41] T. van den Broek, "Formation control of unicycle mobile robots: Theory and experiments," M.S. thesis, Dept. Phys. Eindhoven Univ. Technol., Eindhoven, The Netherlands, 2008.

[42] F. Mondada, M. Bonani, X. Raemy, J. Pugh, C. Cianci, A. Klaptocz, *et al.*, "The e-puck, a robot designed for education in engineering," in *Proc. 9th Conf. Auto. Robot Syst. Competitions*, Castelo Branco, Portugal, 2009, pp. 59–65.

[43] M. Kaltenbrunner and R. Bencina, "ReacTIVision: A computer-vision framework for table-based tangible interaction," in *Proc. 1st Int. Conf. Tangible Embedded Interaction*, Baton Rouge, LA, USA, 2007, pp. 69–74.

Alejandro Alvarez-Aguirre (M'07) received the B.Sc. degree in electronics and communications engineering from the Monterrey Institute of Technology, Mexico, the M.Sc. degree in mechatronics from the Center for Research and Advanced Studies, National Polytechnic Institute, Ciudad de México, Mexico, and the Ph.D. degree in mechanical engineering from the Eindhoven University of Technology, Eindhoven, The Netherlands, in 2003, 2006, and 2011, respectively.

He is currently a Mechatronics Design Engineer with ASML, Veldhoven, The Netherlands. His current research interests include the analysis and control of (non)linear systems subject to time-delays, cooperative control of mobile robots, and online trajectory generation methods for robotic systems.

Nathan van de Wouw (M'08) was born in 1970. He received the M.Sc. (Hons.) and Ph.D. degrees in mechanical engineering from the Eindhoven University of Technology, Eindhoven, the Netherlands, in 1994 and 1999, respectively.

He was with the Department of Mechanical Engineering, Eindhoven University of Technology, Group of Dynamics and Control, as an Assistant Professor or an Associate Professor from 1999 to 2013. In 2000, he was with Philips Applied Technologies, Eindhoven, and the Netherlands Organization for Applied Scientific Research, Delft, The Netherlands, in 2001. He was a Visiting Professor with the University of California Santa Barbara, CA, USA, in 2006 and 2007, the University of Melbourne, Melbourne, Australia, in 2009 and 2010, and the University of Minnesota, Minneapolis, MN, USA, in 2012 and 2013. He has published a large number of journal and conference papers and the books *Uniform Output Regulation of Nonlinear Systems: A convergent Dynamics Approach* with A. V. Pavlov and H. Nijmeijer (Birkhauser, 2005) and *Stability and Convergence of Mechanical Systems with Unilateral Constraints* with R. I. Leine (Springer-Verlag, 2008). His current research interests include the analysis and control of nonlinear/nonsmooth systems and networked control systems.

Prof. van de Wouw is currently an Associate Editor for the journals *Automatica* and the IEEE TRANSACTIONS ON CONTROL SYSTEMS TECHNOLOGY.

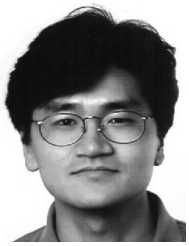

Toshiki Oguchi (M'96) received the B.S., M.S., and Dr.Eng. degrees in mechanical engineering from Tokyo Metropolitan University, Tokyo, Japan, in 1990, 1992, and 1995, respectively.

He was a Research Associate with the Department of Computer Science, National Defense Academy, Kanagawa, Japan, from 1995 to 1997. In 1997, he joined Tokyo Metropolitan University, where he is currently an Associate Professor with the Department of Mechanical Engineering, Graduate School of Science and Engineering. In 2003, 2008, and 2009, he was a Visiting Scientist with the Department of Mechanical Engineering, Eindhoven University of Technology, Eindhoven, The Netherlands. His current research interests include control theory for nonlinear systems with time-delays, control of complex systems, chaos synchronization and nonlinear systems theory.

Henk Nijmeijer (F'00) was born in 1955. He received the M.Sc. and Ph.D. degrees in mathematics from the University of Groningen, Groningen, The Netherlands, in 1979 and 1983, respectively.

He was with the Department of Applied Mathematics, University of Twente, Enschede, the Netherlands, from 1983 to 2000. Since 1997, he has been part-time affiliated with the Department of Mechanical Engineering, Eindhoven University of Technology, Eindhoven, the Netherlands. Since 2000, he has been a Full Professor with Eindhoven University of Technology, and a Chair of the Dynamics and Control Section. He has published a large number of journal and conference papers, and several books, including the classical *Nonlinear Dynamical Control Systems* (Springer, 1990, co-author A. J. van der Schaft), with A. Rodriguez, *Synchronization of Mechanical Systems* (World Scientific, 2003) with R. I. Leine, *Dynamics and Bifurcations of Non-Smooth Mechanical Systems* (Springer-Verlag, 2004), and with A. Pavlov and N. van de Wouw, *Uniform Output Regulation of Nonlinear Systems* (Birkhauser 2005).

Dr. Nijmeijer is an Editor-in-Chief of the *Journal of Applied Mathematics*, a Corresponding Editor of the *SIAM Journal on Control and Optimization*, and a Board Member of the *International Journal of Control*, the *International Journal of Automatica*, the *Journal of Dynamical Control Systems*, the *International Journal of Bifurcation and Chaos*, the *International Journal of Robust and Nonlinear Control*, the *Journal of Nonlinear Dynamics*, and the *Journal of Applied Mathematics and Computer Science*. He was a recipient of the IEE Heaviside premium in 1990. In 2008, the research evaluation of the Dutch Mechanical Engineering Departments, the Dynamics and Control group was evaluated as excellent regarding all aspects (quality, productivity, relevance, and viability). He is an honorary knight of the Golden Feedback Loop, Norwegian University of Science and Technology, Trondheim, Norway. He is a Board Member of the Dutch Institute on Systems and Control, a Council Member of IFAC, and has been an Organizer, and/or the IPC Chair of numerous international conferences and workshops.